Conditions for a return to normal under COVID-19 mitigation measures and vaccinations

Valentina Marziano [1,2,#], Giorgio Guzzetta [1,2,#], Alessia Mammone [3], Flavia Riccardo [4], Piero Poletti [1,2], Filippo Trentini [1,2], Mattia Manica [1,2], Andrea Siddu [3], Paola Stefanelli [4], Patrizio Pezzotti [4], Marco Ajelli [5,6,^], Silvio Brusaferro [4,^], Giovanni Rezza [3,^], Stefano Merler [1,2,^,*]

Affiliations:

1 Center for Health Emergencies, Bruno Kessler Foundation, Trento, Italy

2 Epilab-JRU, FEM-FBK Joint Research Unit, Trento, Italy

3 Ministry of Health, Rome, Italy

4 Istituto Superiore di Sanità, Rome, Italy

5 Department of Epidemiology and Biostatistics, Indiana University School of Public Health, Bloomington, United States

6 Laboratory for the Modeling of Biological and Socio-technical Systems, Northeastern University, Boston, United States

joint first authors

^ joint senior authors

* corresponding author: Stefano Merler, merler@fbk.eu

Abstract

Background: Being unable to suppress SARS-CoV-2 transmission, the majority of countries worldwide have resorted to a mitigation approach, adjusting physical distancing restrictions (PDRs) to find a balance between viral circulation, individual freedoms and economic losses. Vaccination campaigns in many countries are allowing the progressive release of restrictions aimed at reducing infectious contacts.

Methods: We propose a novel mathematical modeling framework where we assume that PDRs are adjusted to maintain an approximately constant incidence, allowing for a progressive resuming of contacts as population immunity accrues. Different scenarios are investigated to evaluate the impact on reopening of critical vaccination parameters, such as the number of daily doses administered, the coverage, the duration of vaccine protection.

Results: We identify five conditions that can allow the complete resuming of pre-pandemic contacts within 9 to 15 months since vaccination start: a sufficiently high coverage (around 75%) and capacity (around 4 daily doses per 1,000 population), a high vaccine efficacy on preventing infections, the availability of a pediatric vaccine, and a long-term duration of protection. If these conditions are met, the two-year cumulative incidence of deaths is expected to remain between 0.43 and 0.77 per 1,000 population. A short-lived vaccine protection will require re-vaccination campaigns, in absence of which a new intensification of PDRs is expected around month 14. Strategies oriented to prioritize the suppression of SARS-CoV-2 by maintaining strict restrictions will not be able to reduce the time to complete reopening, possibly resulting in acceptability issues; on the other hand, we caution that a premature reopening after the vaccination of the most fragile population segments may result in large epidemics with a heavy burden of deaths.

Conclusions: Vaccination programs can allow a return to normal under the identified conditions, but the release of PDRs must be gradual to avoid new epidemic waves and unnecessary deaths.

Background

Since December 2020, vaccinations against COVID-19 are being rolled out in many countries of the world, in a race to put an end to a pandemic that has caused millions of lives lost [1], devastating economic effects [2], and a tremendous impact on mental health [3]. Limitations in the supply of COVID-19 vaccines and in the logistics of rollout imply that several months elapse between the start of immunization campaigns and the acquisition of significant population immunity [4]. Meanwhile, non-pharmaceutical interventions (NPIs) remain the main tool to maintain control of the epidemic. While China and a few other countries in South-East Asia and Oceania have successfully pursued a zero-COVID policy [5] with suppression of transmission via aggressive localized lockdown policies and strict border control, most countries in the world resorted to mitigation strategies [6], adjusting physical distancing restrictions (PDRs) in the attempt to balance a low level of viral circulation with individual freedoms and economic losses. In practice, this balance is not always achieved as desired, resulting in an alternance between periods of constant or declining circulation and new resurgences, to which correspond phases of relaxation and intensification of PDRs. Projecting the impact of vaccination under such unstable conditions is complex and most approaches today have assumed constant restrictions and various degrees of epidemic severity while vaccination is implemented [4, 7-10]. Here, we propose a different framework by simulating the effect of a vaccine rollout assuming that governments will be capable to maintain an approximately constant incidence by adjusting PDRs as immunity accumulates. As population immunity accrues due to natural infection and vaccination, the proportion of allowed contacts will increase until all pre-pandemic contacts are eventually resumed, representing the process of PDRs relaxation.

Results

Vaccination programs under mitigation

As a baseline, we consider a two-dose vaccination campaign with the following assumptions: i) transmissibility of SARS-CoV-2 is assumed to be 50% higher than that of historical lineages, to simulate the dominance of hyper-transmissible viral lineages in many countries [11-17]; ii) an incidence of reported cases maintained at about 50 cases per week per 100,000 population; iii) a vaccination coverage of 75%; iv) a daily capacity of 4 doses per 1,000 population; v) prioritization based on the WHO SAGE roadmap [18] (Appendix); vi) vaccines are administered independently of a previous SARS-CoV-2 infection; vii) vaccines prevent infection; viii) protection is long-lasting. These baseline choices are then modified in a number of alternative scenarios to evaluate a broad range of possible outcomes.

The impact of vaccination is quantified in terms of cumulative deaths and of the relaxation of PDRs. The latter is reported as the percent of resumed contacts, with 0% representing restrictions that were needed to keep a constant incidence at the start of the vaccination program, when more transmissible lineages were not widespread in most countries, and 100% representing complete reopening. We also estimate the potential reproduction number over time, representing the SARS-CoV-2 reproduction number that would be observed if PDRs are completely relaxed at each time. We define as “zero-COVID” a situation in which no cases are reported for at least two consecutive weeks, similarly to what occurs in some countries where circulation is generally suppressed but local flare-ups may occur due to importation of cases (e.g., via outbreaks in under-vaccinated communities). We take Italy as a case study and we simulate a time horizon of two years.

In the absence of vaccination and under mitigation measures, we estimate 1.71 cumulative COVID-19 deaths per 1,000 population (95%CI: 0.94-2.89) over the two years (Figure 1A). To maintain a constant incidence, PDRs should remain stricter than those required at the beginning of vaccination (represented by negative values of the PDRs relaxation in Figure 1A-B) throughout the two years, due to the increased transmissibility of the dominant B.1.1.7 lineage [11-17]. Furthermore, a large potential for new epidemic waves would remain at the end of the two years, with a potential reproduction number estimated at 2.1-2.4 (Figure 1C). These results suggest that in the absence of vaccination, the only viable way to control COVID-19 would be to maintain very strict PDRs in the very long term.

In the baseline scenario, the vaccination campaign is expected to be completed after about 13 months. Vaccination can limit cumulative deaths to 0.61 per 1,000 (95%CI: 0.34-1.03), i.e., almost 65% less than in absence of vaccination (Figure 1A). In addition, PDRs might be completely relaxed by month 13 (Figure 1B), when the potential reproduction number is expected to fall below the epidemic threshold (Figure 1C). The majority of relaxations is to be expected over months 9-12 since the start of vaccination (Figure 1B).

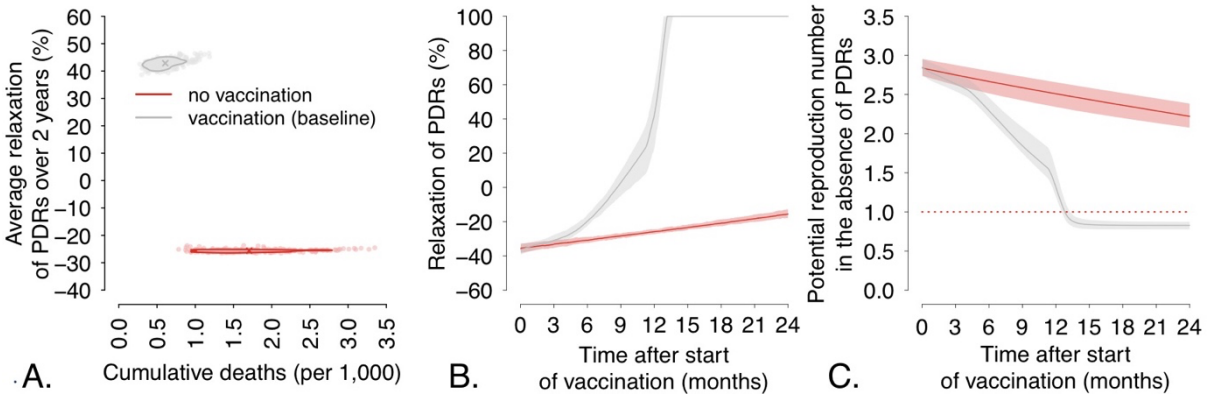

Figure 1. Model projections for mitigation scenarios with and without vaccination. A) Comparison between scenarios in terms of the cumulative incidence of deaths and the average relaxation of PDRs over the two simulated years. Individual stochastic simulations are shown as points, the mean of their bivariate distribution as crosses and its 75-percentile as closed curves. B) Relaxation of PDRs over time. Solid lines indicate the median, shaded areas the 95% projection interval. C) Potential reproduction number over time. Solid lines indicate the median, shaded areas the 95% projection interval. The horizontal dashed red line indicates the epidemic threshold.

The effect of a vaccination campaign may depend on several factors. Some of these depend on organizational and public health choices, e.g., how fast available vaccine doses are administered. A halved vaccination capacity (2 daily doses per 1,000 population) would imply completing the program after over 2 years, resulting in a higher mortality compared to the baseline (0.89 per 1,000; 95%CI: 0.50-1.52) and in a slower relaxation of PDRs, which is expected to be completed only by month 23 (95%CI: 22-24, Figure 2A). Vaccination capacities higher than the baseline would have a limited impact on the burden of deaths (10% reduction from the baseline at most), but they would allow a quicker relaxation of PDRs, reaching complete reopening at month 10 and 9 for vaccination capacities of 6 and 8 daily doses per 1,000 population, respectively.

The population's willingness to be vaccinated is represented by the achievable coverage. A 60% coverage would initially anticipate the relaxation of PDRs by switching earlier from high-risk to high-transmission population segments, but it would result in about 1.36 cumulative deaths per 1,000

population (95%CI: 0.77-2.21, Figure 2B) and in a later completion of reopening (not before month 19, and within 2 years in 84% of simulations only). Conversely, an increased coverage to 90% would reduce the mortality burden to 0.43 per 1,000 (95%CI: 0.25-0.75), leading to a zero-COVID scenario by month 20-23. However, the complete relaxation of PDRs would be slightly delayed to month 14 or 15.

One of the main unknowns on vaccine performance is the duration of vaccine protection. When assuming that protection wanes on average between 6 and 24 months after administration, in absence of a re-vaccination campaign we estimate 1.57-1.78 deaths per 1,000 population in two years (with a wide uncertainty ranging from 0.88 to 2.99 per 1,000, Figure 2C), and the need to reinstate stricter PDRs starting around month 14 to counter the rising reproduction number of SARS-CoV-2 driven by the refueling of the susceptible reservoir (Figure 2C). We note however that the end of the vaccination campaign around month 13 in the baseline scenario implies that even with a short duration of vaccine protection, re-vaccination is feasible before the deterioration of the epidemiological situation, if vaccine stockpiles/supplies are sufficient.

Another uncertainty in the evolving epidemiology of COVID-19 is the transmissibility of SARS-CoV-2 variants [10-16]. To account for these uncertainties, we considered transmissibility values that are 30% to 70% higher compared to estimates for historical lineages of SARS-CoV-2. In the case of a transmissibility increase of 70%, the expected cumulative incidence of deaths would rise to 0.77 per 1,000 population (95%CI 0.40-1.27) (Figure 2D) and the time of complete reopening would be expected between month 14 and 17. Considering also an increased lethality of the variants [19-20], a cumulative mortality of 1.00 per 1,000 (95%CI 0.56-1.69) might be expected (see Appendix).

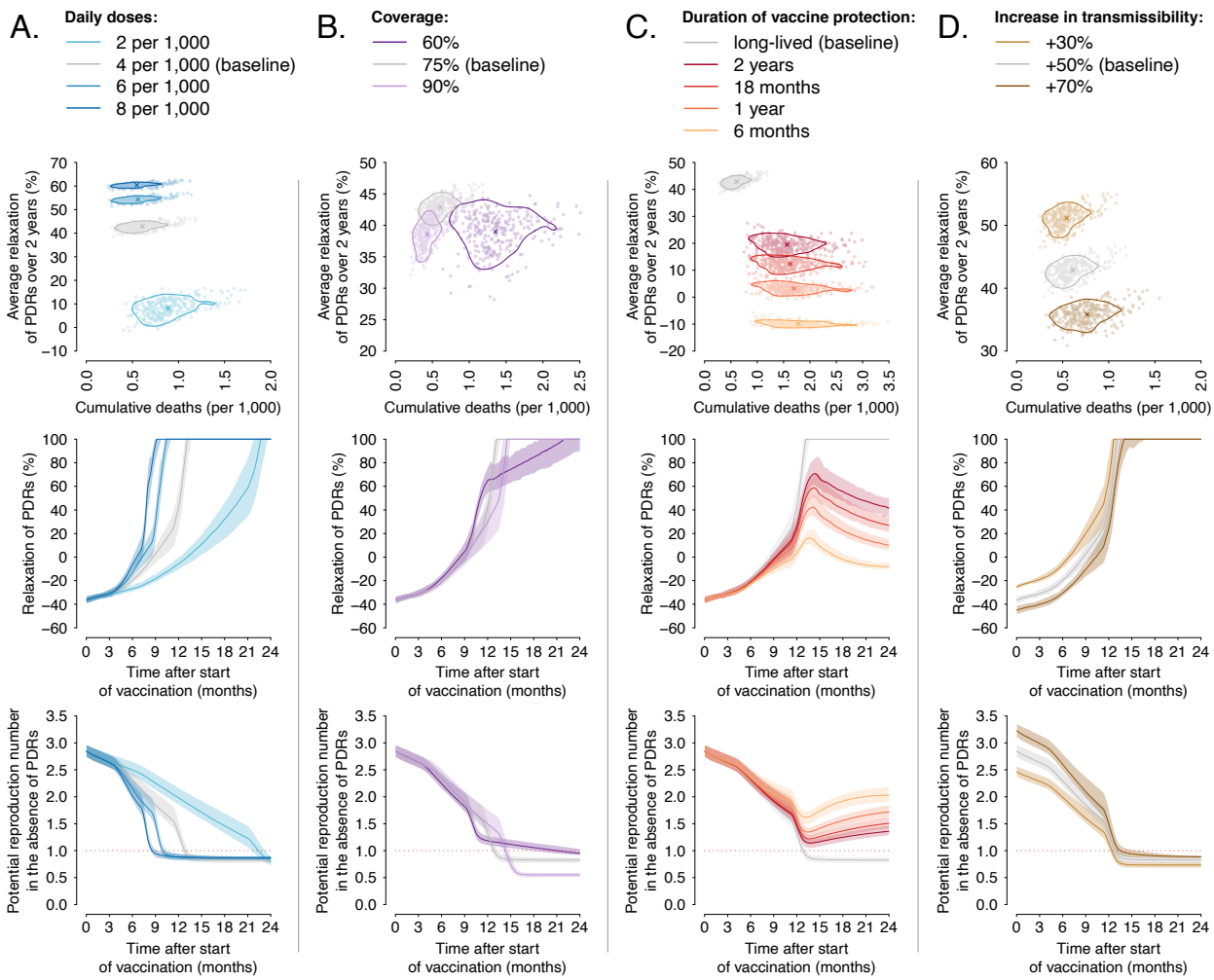

Figure 2. Alternative vaccination scenarios. A) vaccination capacity; B) vaccine coverage; C) duration of vaccine protection; D) Increase of transmissibility with respect to historical lineages. Top panels compare scenarios using the cumulative incidence of deaths and the average relaxation of PDRs over the two simulated years. Individual stochastic simulations are shown as points, the mean of their bivariate distribution as crosses and its 75-percentile as closed curves. Middle panels show the PDRs relaxation over time. Solid lines indicate the median, shaded areas the 95% projection interval. Bottom panels show the potential reproduction number over time. Solid lines indicate the median, shaded areas the 95% projection interval. The horizontal dashed red line indicates the epidemic threshold.

We evaluated the sensitivity of model outputs with respect to several other variables (Appendix). When allowing incidence levels higher than 50 weekly reported cases per 100,000, the accumulation of immunity from natural infections speeds up the relaxation of PDRs but the death burden increases proportionally to the incidence level. If a pediatric vaccine will not be made available by the time that age groups above 15 years have been covered (around month 11 in the baseline), the projected deaths may increase by 40% and the date of complete reopening may become highly uncertain (between month 13 and month 24 or later), but a large majority of contacts may still be resumed in the second year since vaccination. Prioritizing age groups different from the elderly would result in large increases in mortality, without major advantages in the time to complete relaxation. When considering a vaccine efficacy reduced by 15%, we estimate an over two-fold burden of deaths, and the time to complete relaxation of PDRs is put off by about 9 months. If the vaccine provides protection against disease, but not against infection, we expect 15% more deaths at the end of the

two years but maintaining PDRs in the long term would be necessary, as in a scenario without vaccination. A homogeneous susceptibility to infection (rather than reduced in children and increased in older adults [21-22]) would reduce deaths by 40%. Finally, model results were substantially insensitive to uncertainties in the value of initial immunity.

Alternative strategies: SARS-CoV-2 suppression or early reopening

Governments may choose to use the population immunity conferred by vaccines to achieve zero-COVID sooner by not lifting PDRs until no locally acquired infections are reported. When no relaxation of PDRs is allowed since the start of vaccination, we estimate a cumulative incidence of 0.21 deaths per 1,000 population (95%CI: 0.12-0.33) for this scenario, roughly one third than the baseline (Figure 3A). Zero-COVID could be reached at month 13 since vaccination start (95%CI: 12-15), after which complete reopening would be feasible. However, the potential reproduction number would still be hovering above the epidemic threshold (median 1.03, 95%CI 0.99-1.07), implying that outbreaks would still be likely not only in under-vaccinated pockets of the population but also on a broader scale.

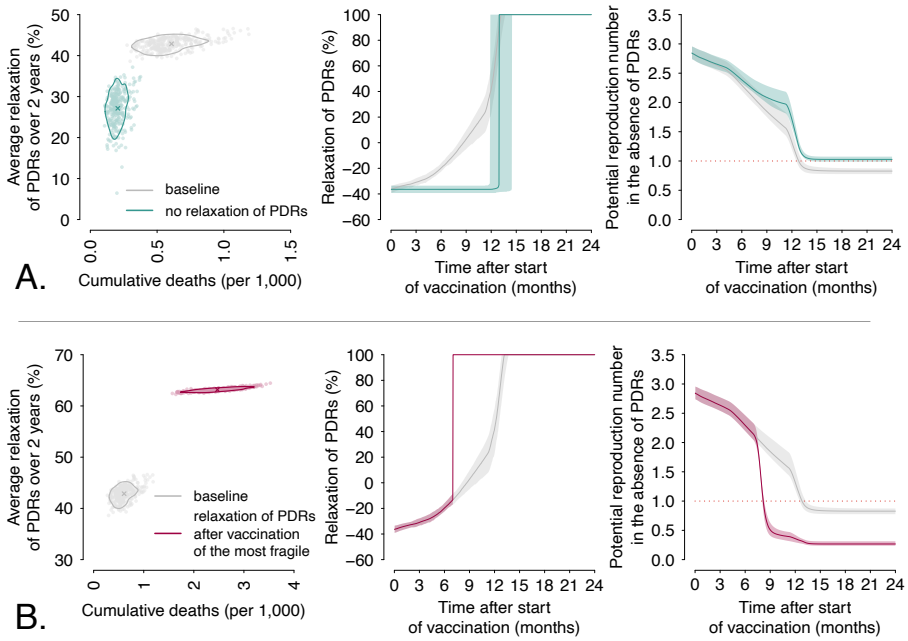

Figure 3. Increased transmissibility and alternative reopening strategies. A) strategy aimed at earlier suppression of COVID-19 transmission; B) complete reopening after immunization of the most fragile. Left compare scenarios using the cumulative incidence of deaths and the average relaxation of PDRs over the two simulated years. Individual stochastic simulations are shown as points, the mean of their bivariate distribution as crosses and its 75-percentile as closed curves. Center panels show the PDRs relaxation over time. Solid lines indicate the median, shaded areas the 95% projection interval. Right panels show the potential reproduction number over time. Solid lines indicate the median, shaded areas the 95% projection interval. The horizontal dashed red line indicates the epidemic threshold.

An opposite strategy might be to maintain mitigation measures only until the most fragile population segments (individuals above 60 years of age or with comorbidities) have been protected. We simulate a scenario where all PDRs are completely removed after this milestone, occurring around month 6 since vaccination start under baseline assumptions. The high potential reproduction number at that

date (2.15, 95%CI 2.05-2.33) would lead to a very large epidemic that may cause a cumulative incidence of 2.47 per 1,000 death (95%CI: 1.71-3.25, Figure 3B) if uncontrolled, even despite the protection of highest-risk populations.

A summary comparison of key results for all considered scenarios is represented in Figure 4.

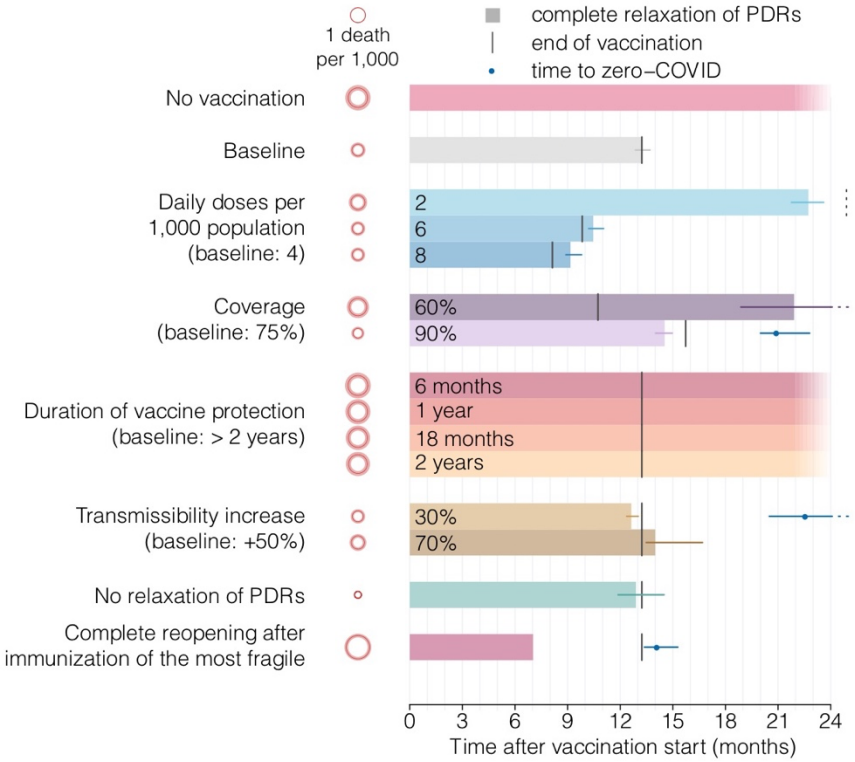

Figure 4. Summary comparison of considered scenarios. Red circles show the mean estimated mortality burden over the two years, with shaded areas representing the 95% projection intervals. Vertical black lines indicate the end of vaccination programs (fixed, given capacity and coverage). A dashed vertical line indicate completion after 24 months. Bars show the median time at which a complete relaxation of PDRs is reached and horizontal lines the 95% projection interval. Fading bars indicate no complete relaxation of PDRs within 24 months. For the scenario with 60% coverage, 84% of simulations resulted in complete relaxation of PDRs before month 24 (dashed horizontal lines). Blue points and horizontal blue lines indicate the median time to zero-COVID and 95% projection interval. When these are not shown, zero-COVID occurs beyond 24 months. For the scenario with 30% transmissibility increase, 79% of simulations resulted in zero-COVID within 24 months (dashed horizontal lines).

Discussion

We examined the effect of COVID-19 vaccination programs in countries which were not able, to date, to suppress the circulation of the virus, assuming that the mitigation approach adopted until now would be maintained throughout the program. The combination of vaccine roll-out and effective mitigation strategies is expected to prevent a large proportion of deaths while at the same time allowing a progressive lifting of physical distancing restrictions. A complete return to a pre-pandemic lifestyle can be expected between 9 and 15 months since the start of vaccination (Figure 4) only if a number of conditions are simultaneously met: first, that a vaccination capacity of at least 4 doses per 1,000 population per day is maintained throughout the program; second, that a population coverage

close to 75% is achieved in all age classes; third, that immunity conferred by vaccines is long-lived; fourth, that vaccines are at highly effective in preventing infection; fifth, that a pediatric vaccine is licensed before the end of the campaign. While the first two conditions are entirely determined by public health actions, the remaining ones depend on factors that are still uncertain. A key role will be played by the duration of immunity conferred by the licensed vaccines; if it will be short-lived, re-vaccination must be considered as an option, as soon as the primary campaign is over. Alternatively, the relaxation of PDRs will need to be reversed at some point with a dramatic rise in the number of deaths. This aspect reinforces the importance of vaccination capacities of at least 4 daily doses per 1,000, which would allow to start a re-vaccination campaign within 13-15 months, i.e., approximately when the effect of waning vaccine immunity would require a tightening of restrictions. The high efficacy of vaccines in preventing infections seems to be demonstrated for at least some of the licensed vaccines [23-26]; however, it needs to be further confirmed also for other vaccines under approval and with respect to circulating and future emerging variants. If vaccines only avoided symptomatic disease with no reduction in susceptibility or infectiousness, our simulations suggest a dramatically different outcome of the campaign, especially in terms of the ability of countries to relax PDRs. Finally, the expectation of having an effective pediatric vaccine against SARS-CoV-2 in the second half of the year, as assumed in the baseline analysis, is not unrealistic, since several manufacturers have already started phase 2/3 trials for children as young as 3 years old [27]. However, if the extension of the vaccination program to children will not be feasible, a majority of pre-pandemic contacts may still be resumed after one year since vaccination, but the time to complete PDR relaxation would be significantly delayed and a 40% increase in the number of deaths may be expected.

Besides analyzing the scenarios with a pure mitigation approach, we evaluated the possibility that countries will not relax PDRs, using the buildup of population immunity to pursue suppression of transmission. In this case, zero-COVID can be obtained in about 13 months, after which the transmission potential will have reached values close to the epidemic threshold and a complete reopening may be allowed. This suppression-oriented approach would reduce by two-thirds the burden of deaths, requiring a similar time until complete reopening than the mitigation approach. However, the tradeoff here is the need to maintain restrictions for a very long period (in general, more than a year), with negative effects on the economy and population's mental health and likely acceptability issues for the public, faced with a declining incidence and mortality. On the opposite, pressures to reopen society are to be expected after the daily incidence of deaths will have dropped to lower values due to the vaccination of the most fragile. We show that if social contacts are completely resumed after the vaccination of individuals with co-morbidities or older than 60 years (i.e., about 6 months into the vaccination program), a major epidemic is to be expected with a very large death toll if left uncontrolled.

There are a number of limitations that must be kept in mind when interpreting these results. First, we did not explicitly model which PDRs are relaxed as vaccination progresses; instead, we assumed a generic relaxation of measures that impacts all ages proportionally. The age-specific effect of relaxing existing PDRs is extremely hard to quantify, and their prioritization is a peculiarly political decision, depending on the governments' strategic interests. Second, we assume mitigation measures to maintain an approximately constant incidence; although this dynamic is clearly idealized, we consider this an acceptable approximation of the fluctuating incidence observed in most countries. We anticipate that possible resurgences due to imperfect mitigation will contribute to speed up the

population immunity and therefore the relaxation of PDRs, however at the cost of more lives lost. Third, we did not explicitly model the effect of other possible features of emerging variants, such as reductions in vaccine efficacy [28-29] or the ability to escape natural immunity [15-16, 30-31], or a combination of them. We estimate that a 15% lower efficacy of vaccines with respect to the one observed against historical lineages and B.1.1.7 [26] would more than double the expected deaths and delay by about 9 months the time to a complete relaxation of PDRs, although a majority of contacts may still be resumed by month 13. The possibility of escape from natural immunity is not expected to be a major driver of our conclusions, considering the limited share of population immunity due to natural infection even in scenarios without vaccination (up to 30% at the end of the two years) and to the fact that vaccination is administered independently of a previous COVID-19 infection [32]. Similar considerations apply to the possibility that immunity from natural infection wanes over time [33]. Fourth, we did not consider possible changes in viral transmissibility due to seasonality, such as the closure of schools or the larger amount of time spent outdoors during the summer. This may help reduce deaths and expand the margins for reopening during the summer.

There are still many uncertainties on characteristics of vaccines and on the evolving epidemiology of COVID-19. However, we show that vaccination programs under mitigation scenarios may allow a return to normal within approximately one year under certain conditions. However, the ecological interactions [15] and epidemiological characteristics of emerging variants, especially with respect to their increased transmissibility and the efficacy of vaccines, will need to be closely monitored to promptly reassess these conclusions as more evidence will become available.

Methods

We developed an age-structured stochastic model for SARS-CoV-2 transmission and vaccination, based on a susceptible-infectious-removed (SIR) scheme. The population is stratified in 17 5-year age groups from 0 to 84 years plus one age group for individuals aged 85 years or older, and according to the presence/absence of comorbidities. Mixing patterns are assumed to be heterogeneous across ages according to an age-specific social contact matrix [34]. Incidence is maintained approximately constant over time during vaccine rollout by continuously recalibrating a scaling factor on contacts, roughly representing the proportion of pre-pandemic contacts allowed by existing PDRs at each time. We assumed an age-dependent susceptibility to SARS-CoV-2 infection: lower in children under 15 years of age and higher for the elderly (65+), compared to individuals of working age [22]. Asymptomatic and symptomatic individuals are assumed to be equally infectious [22, 35] and infectiousness was also assumed to be the same across age groups [22, 35]. We simulate a two-dose vaccination campaign, in which all individuals are considered eligible for vaccination, independently of a previous diagnosis of infection with SARS-CoV-2. Vaccination is assumed to reduce individuals' susceptibility to SARS-CoV-2 infection, and we assume that vaccine-induced protection is long-lived (i.e., no waning in the two-year time horizon of simulations). Full model details are reported in Appendix.

Competing interest and funding

M.A. has received research funding from Seqirus. The funding is not related to COVID-19. All other authors declare no competing interest. V.M., G.G., P.Po., F.T., M.M. and S.M. acknowledge funding from EU grant 874850 MOOD (catalogued as MOOD 000). V.M., G.G., P.Po., and S.M. acknowledge funding from the VRT

Foundation Trento project COVIDVAX. The contents of this publication are the sole responsibility of the authors and don't necessarily reflect the views of the funders.

References

1. WHO coronavirus (COVID-19) dashboard. https://covid19.who.int/. Accessed on Mar 15, 2021.
2. McKibbin W and Fernando R. The economic impact of COVID-19 (2020). Economics in the Time of COVID-19, 45.
3. Pfefferbaum B and North CS. Mental health and the Covid-19 pandemic. New England Journal of Medicine 2020, 383(6), 510-512.
4. Bubar KM, Reinholt K, Kissler SM, Lipsitch M, Cobey S, Grad YH and Larremore DB. Model-informed COVID-19 vaccine prioritization strategies by age and serostatus. Science 2021, 371(6532), 916-921.
5. Baker MG, Wilson N and Blakely T. Elimination could be the optimal response strategy for COVID-19 and other emerging pandemic diseases. BMJ 2020, 371.
6. Flaxman S, Mishra S, Gandy A, Unwin HJT, Mellan TA, Coupland H et al. Estimating the effects of non-pharmaceutical interventions on COVID-19 in Europe. Nature 2020, 584(7820), 257-261.
7. Yang J, Marziano V, Deng X, Guzzetta G, Zhang J, Trentini F, et al. Can a COVID-19 vaccination program guarantee the return to a pre-pandemic lifestyle? (2021) medRxiv: https://www.medrxiv.org/content/10.1101/2021.02.03.21251108v1 . Accessed Mar 15, 2021
8. Moore S, Hill EM, Dyson L, Tildesley M and Keeling MJ. Modelling optimal vaccination strategy for SARS-CoV-2 in the UK. medRxiv, 2020. Available at https://www.medrxiv.org/content/10.1101/2020.09.22.20194183v2 . Accessed Mar 15, 2021.
9. Bosetti P, Tran Kiem C, Andronico A, Paireau J, Levy Bruhl D, Lina B et al. A race between SARS-CoV-2 variants and vaccination: The case of the B.1.1.7 variant in France. Available at https://hal-pasteur.archives-ouvertes.fr/pasteur-03149525 . Accessed Mar 15, 2021.
10. MacIntyre CR, Costantino V and Trent MJ. Modelling of COVID-19 vaccination strategies and herd immunity, in scenarios of limited and full vaccine supply in NSW, Australia. medRxiv, 2020. Available at https://www.medrxiv.org/content/10.1101/2020.12.15.20248278v2.abstract . Accessed Mar 15, 2021.
11. Davies NG, Abbott S, Barnard RC, Jarvis CI, Kucharski AJ, Munday JD, et al. Estimated transmissibility and impact of SARS-CoV-2 lineage B.1.1.7 in England. Science, 2021.
12. Volz E, Mishra S, Chand M, Barrett JC, Johnson R, Geidelberg L, et al. Assessing transmissibility of SARS-CoV-2 lineage B. 1.1. 7 in England. Nature. 2021 Mar 25:1-7.
13. Galloway SE, Paul P, MacCannell DR, Johansson MA, Brooks JT, MacNeil A, et al. Emergence of SARS-CoV-2 B.1.1.7 lineage—United States, December 29, 2020 – January 12, 2021. Morbidity and Mortality Weekly Report. 2021 Jan 22;70(3):95.
14. Gaymard A, Bosetti P, Feri A, Destras G, Enouf V, Andronico A, et al. Early assessment of diffusion and possible expansion of SARS-CoV-2 Lineage 20I/501Y. V1 (B. 1.1. 7, variant of concern 202012/01) in France, January to March 2021. Euro Surveill 2021 Mar 4;26(9):2100133.
15. Stefanelli P, Trentini F, Guzzetta G, Marziano V, Mammone A, Poletti P, et al. Co-circulation of SARS-CoV-2 variants B. 1.1. 7 and P. 1. medRxiv, 2021. Available at https://www.medrxiv.org/content/10.1101/2021.04.06.21254923v1
16. Faria NR, Mellan TA, Whittaker C, Claro IM, Candido D, Mishra S, et al. Genomics and epidemiology of the P.1 SARS-CoV-2 lineage in Manaus, Brazil. Science, 2021.
17. European Center for Disease Control. Rapid Risk Assessment. SARS-CoV-2 - increased circulation of variants of concern and vaccine rollout in the EU/EEA,14th update. Available at https://www.ecdc.europa.eu/sites/default/files/documents/RRA-covid-19-14th-update-15-feb-2021.pdf . Accessed on Mar 15, 2021

18. WHO SAGE roadmap for prioritizing uses of COVID-19 vaccines in the context of limited supply. https://www.who.int/docs/default-source/immunization/sage/covid/sage-prioritization-roadmap-covid19-vaccines.pdf?Status=Temp&sfvrsn=bf227443_2. Accessed March 15, 2021.
19. Challen R, Brooks-Pollock E, Read JM, Dyson L, Tsaneva-Atanasova K, Danon L. Risk of mortality in patients infected with SARS-CoV-2 variant of concern 202012/1: matched cohort study. BMJ 2021; 372:n579
20. Davies NG, Jarvis CI, CMMID COVID-19 Working Group, Edmunds WJ, Jewell NP, Diaz-Ordaz K, Keogh RH. Increased mortality in community-tested cases of SARS-CoV-2 lineage B.1.1.7. Nature, 2021; https://doi.org/10.1038/s41586-021-03426-1
21. Viner RM, Mytton OT, Bonell C, Melendez-Torres GJ, Ward J, Hudson L, Waddington C, Thomas J, Russell S, van der Klis F, Panovska-Griffiths J. Susceptibility to SARS-CoV-2 infection among children and adolescents compared with adults: a systematic review and meta-analysis. JAMA pediatrics, 175(2), 143-156.
22. Hu S, Wang W, Wang Y et al. Infectivity, susceptibility, and risk factors associated with SARS-CoV-2 transmission under intensive contact tracing in Hunan, China. Nat Commun 2021, 12: 1533.
23. Amit S, Regev-Yochay G, Afek A, Kreiss Y and Leshem E. Early rate reductions of SARS-CoV-2 infection and COVID-19 in BNT162b2 vaccine recipients. The Lancet 2021, 397(10277), 875-877.
24. Hall VJ, Foulkes S, Saei A, Andrews N, Oguti B, Charlett A et al. Effectiveness of BNT162b2 mRNA Vaccine Against Infection and COVID-19 Vaccine Coverage in Healthcare Workers in England, Multicentre Prospective Cohort Study (the SIREN Study). SSRN preprint, 2021. Available at https://papers.ssrn.com/sol3/papers.cfm?abstract_id=3790399 . Accessed Mar 15, 2021.
25. Tande A, Pollock B, Shah ND, Farrugia G, Virk A, Swift M et al. Impact of the COVID-19 Vaccine on Asymptomatic Infection Among Patients Undergoing Pre-Procedural COVID-19 Molecular Screening. Clinical Infectious Diseases, 2021; ciab229.
26. Dagan N, Barda N, Kepten E, Miron O, Perchik S, Katz MA, et al. BNT162b2 mRNA Covid-19 vaccine in a nationwide mass vaccination setting. New England Journal of Medicine, 2021.
27. Aschwanden, C. Five reasons why COVID herd immunity is probably impossible. Nature News, March 18, 2021. Nature 2021; 591: 520-522.
28. Fontanet A, Autran B, Lina B, Kieny MP, Karim SSA and Sridhar D. SARS-CoV-2 variants and ending the COVID-19 pandemic. The Lancet, 2021.
29. Collier DA, De Marco A, Ferreira IA, Meng B, Datir R, Walls AC et al. SARS-CoV-2 B. 1.1. 7 sensitivity to mRNA vaccine-elicited, convalescent and monoclonal antibodies. Nature, 2021.
30. Greaney AJ, Loes AN, Crawford KH, Starr TN, Malone KD, Chu HY and Bloom JD. Comprehensive mapping of mutations in the SARS-CoV-2 receptor-binding domain that affect recognition by polyclonal human plasma antibodies. Cell host & microbe 2021.
31. Wang P, Nair MS, Liu L, Iketani S, Luo Y, Guo Y et al. Antibody Resistance of SARS-CoV-2 Variants B. 1.351 and B.1.1.7. Nature 2021.
32. Prendecki M, Clarke C, Brown J, Cox A, Gleeson S, Guckian M, et al. Effect of previous SARS-CoV-2 infection on humoral and T-cell responses to single-dose BNT162b2 vaccine. The Lancet, 2021.
33. Hall V, Foulkes S, Charlett A, Atti A, Monk EJ, Simmons R et al. Do antibody positive healthcare workers have lower SARS-CoV-2 infection rates than antibody negative healthcare workers? Large multi-centre prospective cohort study (the SIREN study), England: June to November 2020. medRxiv, 2021. Available at https://www.medrxiv.org/content/10.1101/2021.01.13.21249642v1 . Accessed Mar 15, 2021.
34. Mossong J, Hens N, Jit M, Beutels P, Auranen K, Mikolajczyk R, et al. Social contacts and mixing patterns relevant to the spread of infectious diseases. PLoS Med. 2008 Mar 25;5(3):e74.
35. Sun K, Wang W, Gao L, Wang Y, Luo K, Ren L, et al. Transmission heterogeneities, kinetics, and controllability of SARS-CoV-2. Science. 2021 Jan 15;371(6526). https://doi.org/10.1126/science.abe2424

APPENDIX

Conditions for a return to normal under COVID-19 mitigation measures and vaccinations

Valentina Marziano [1,2,#], Giorgio Guzzetta [1,2,#], Alessia Mammone [3], Flavia Riccardo [4], Piero Poletti [1,2], Filippo Trentini [1,2], Mattia Manica [1,2], Andrea Siddu [3], Paola Stefanelli [4], Patrizio Pezzotti [4], Marco Ajelli [5,6,^], Silvio Brusaferro [4,^], Giovanni Rezza [3,^], Stefano Merler [1,2,^,*]

Affiliations:

[1] Center for Health Emergencies, Bruno Kessler Foundation, Trento, Italy
[2] Epilab-JRU, FEM-FBK Joint Research Unit, Trento, Italy
[3] Ministry of Health, Rome, Italy
[4] Istituto Superiore di Sanità, Rome, Italy
[5] Department of Epidemiology and Biostatistics, Indiana University School of Public Health, Bloomington, United States
[6] Laboratory for the Modeling of Biological and Socio-technical Systems, Northeastern University, Boston, United States

joint first authors
^ joint senior authors
* corresponding author: Stefano Merler, merler@fbk.eu

Contents

1. Materials and Methods 13
1.1 Model for SARS-CoV-2 transmission and vaccination 13
1.2 Implementing perfect mitigation 15
1.3 Model initialization 16
1.4 Computation of age-specific vaccination rates over time 17
1.5 Model outputs 19
2. Sensitivity analyses 20
2.1 Vaccination capacity 21
2.2 Priority population 23
2.3 Vaccine coverage 26
2.4 Duration of vaccine protection 27
2.5 Increased mortality 28
2.6 Complete reopening after vaccination of the most fragile 28
2.7 Incidence level of reported cases 29
2.8 Vaccine efficacy 29
2.9 Homogeneous susceptibility 30
2.10 Vaccine protection 30
2.11 Initial immunity 32
References 33

1. Materials and Methods

1.1 Model for SARS-CoV-2 transmission and vaccination

We developed an age-structured stochastic model for SARS-CoV-2 transmission and vaccination, based on a susceptible-infectious-removed (SIR) scheme. Mixing patterns are assumed to be heterogeneous across ages according to an age-specific social contact matrix [1,2]. In the main analysis, we assume an age-dependent susceptibility to SARS-CoV-2 infection: lower in children under 15 years of age and higher for the elderly (65+), compared to individuals of working age [3]. The case of a homogeneous susceptibility to infection in all age groups is explored as sensitivity analysis (see Section 2.9).

We simulate a two-dose vaccination campaign. In the baseline analysis, vaccination is assumed to reduce individuals' susceptibility to SARS-CoV-2 infection, and we assume that vaccine-induced protection lasts longer the time horizon considered (2 years). The case of a vaccine with a protection that wanes on average 2 years, 18 months, 1 year or 6 months after administration, and of a vaccine providing protection against disease, but not infection, are explored as sensitivity analyses (see Section 2.4 and 2.10, respectively).

The baseline model is described by the following system of differential equations (summarized by the schematic representation in Figure S1):

$$
\begin{cases}
S'_{a,c}(t) = -\lambda_a(t)S_{a,c}(t) - \alpha_{a,c}(t)S_{a,c}(t) \\
I'_{a,c}(t) = \lambda_a(t)S_{a,c}(t) - \gamma I_{a,c}(t) - \alpha_{a,c}(t)I_{a,c}(t) \\
R'_{a,c}(t) = \gamma I_{a,c}(t) - \alpha_{a,c}(t)R_{a,c}(t) \\
U'_{a,c}(t) = \alpha_{a,c}(t)(I_{a,c}(t) + R_{a,c}(t)) \\
V'_{0,a,c}(t) = \alpha_{a,c}(t)S_{a,c}(t) - (1 - VE_{0,a})\lambda_a(t)V_{0,a,c} - \omega_0 V_{0,a,c}(t) \\
V'_{1,a,c}(t) = \omega_0 V_{0,a,c}(t) - (1 - VE_{1,a})\lambda_a(t)V_{1,a,c} - \omega_1 V_{1,a,c}(t) \\
V'_{2,a,c}(t) = \omega_1 V_{1,a,c}(t) - (1 - VE_{2,a})\lambda_a(t)V_{2,a,c} - \omega_2 V_{2,a,c}(t) \\
V'_{3,a,c}(t) = \omega_2 V_{2,a,c}(t) - (1 - VE_{3,a})\lambda_a(t)V_{3,a,c} \\
I^{V\prime}_{a,c}(t) = \lambda_a(t)[(1 - VE_{0.a})V_{0,a,c} + (1 - VE_{1,a})V_{1,a,c} + (1 - VE_{2,a})V_{2,a,c} + (1 - VE_{3,a})V_{3,a,c}] - \gamma I^V_{a,c}(t) \\
R^{V\prime}_{a,c}(t) = \gamma I^V_{a,c}(t)
\end{cases}
$$

where:

- the population class {a,c} represents individuals in age group a and in underlying conditions status c ("with" or "without");
- $S_{a,c}$ represents the number of unvaccinated individuals in the population class {a,c} who are fully susceptible to SARS-CoV-2 infection;
- $I_{a,c}$ represents the number of infectious unvaccinated individuals in the population class {a,c}.
- $R_{a,c}$ represents the number of unvaccinated individuals in the population class {a,c} who recovered from infection.
- $U_{a,c}$ represents the number of individuals in the population class {a,c} who are vaccinated despite having already experienced SARS-CoV-2 infection.
- $V_{0,a,c}$; $V_{1,a,c}$; $V_{2,a,c}$ and $V_{3,a,c}$ represent the number of vaccinated individuals at different stages of protection. In particular,
    1) $V_{0,a,c}$ denotes individuals in the population class {a,c} vaccinated with the first dose, for whom the first dose is not effective yet.
    2) $V_{1,a,c}$ denotes individuals in the population class {a,c} vaccinated with the first dose, for whom the first dose is effective.
    3) $V_{2,a,c}$ denotes individuals in the population class {a,c} vaccinated with the second dose for whom the second dose is not effective yet.
    4) $V_{3,a,c}$ denotes individuals in the population class {a,c} vaccinated with the second dose for whom the 2nd dose is effective.
- $I^V_{a,c}$ represents the number of infectious individuals in the population class {a,c} among those who have already received at least one vaccine dose.
- $R^V_{a,c}$ represents the number of individuals in the population class {a,c} who recovered from an infection contracted after having received at least one vaccine dose.

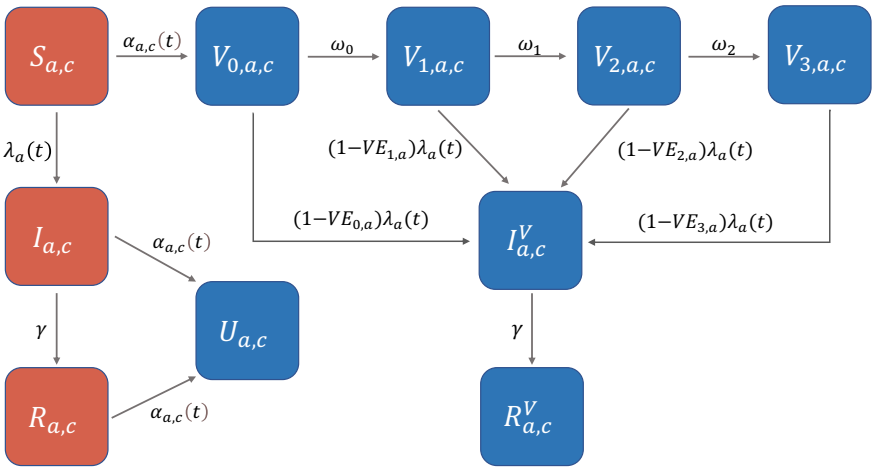

Figure S1. Schematic representation of the baseline model. Red compartments represent unvaccinated individuals and therefore eligible for vaccination; blue compartments represent vaccinated individuals. Model parameters include: the time- and age-dependent force of infection $\lambda_a(t)$; the recovery rate from infection (γ); the time-, age- and group-dependent probability of being vaccinated $\alpha_{a,c}(t)$; the interval between administration of the first dose and full protection by the first dose ($1/\omega_0$); the interval between full protection of the first dose and administration of the second dose ($1/\omega_1$); the interval between administration of the second dose and full protection of the 2nd dose ($1/\omega_2$); age-dependent vaccine efficacies in the different stages *I* of vaccine protection (i=0,1,2,3) are denoted by $VE_{i,a}$.

Susceptible individuals are exposed to a time and age-dependent force of infection $\lambda_a(t)$ which is defined as:

$$\lambda_a(t) = \beta(1+\theta)(1-\varphi)\,\delta(t) r_a \sum_{\tilde{a}} C_{a,\tilde{a}} \frac{\sum_c [I_{\tilde{a},c}(t) + I^V_{\tilde{a},c}(t)]}{\sum_c N_{\tilde{a},c}}$$

where:

- β is a scaling factor shaping SARS-CoV-2 transmissibility in the absence of physical distancing restrictions (PDRs) and other non-pharmaceutical interventions (NPIs) such as face masks or hand hygiene precautions, computed by assuming R_0=3 [4, 5], as estimated for historical lineages of SARS-CoV-2.
- θ is a coefficient representing the transmissibility increase of B.1.1.7 lineage with respect to historical lineages [6-10]. In the baseline analysis, θ is assumed to be 50%; values of θ = 30%, 70% are explored in alternative scenarios.
- $(1-\varphi)$ is a coefficient representing the reduction in the per-contact transmission probability ascribable to NPIs different from PDRs, such as face masks or hand hygiene precautions. We assumed $\varphi = 20\%$ [4, 5].
- $\delta(t) \in \{0,1\}$ is a scaling factor tuning the proportion of pre-pandemic contacts allowed by existing PDRs.
- r_a is the relative susceptibility to SARS-CoV-2 infection at age a: r_a=0.58 (95%CI 0.34-0.98) under 15 years of age; r_a =1 between 15 and 64 years; and r_a=1.65 (95%CI 1.03-2.65) above 64 years [3].
- $C_{a,\tilde{a}}$ represents the age-group-specific contact matrix, whose entries describe the mean numbers of persons in age group $\tilde{a}$ encountered by an individual of age group a per day [1, 2].
- $N_{\tilde{a},c}$ represents the number of individuals in the population class $\{\tilde{a},c\}$, where $\tilde{a}$ represents age and *c* identifies the presence/absence of comorbidities.

For all infectious compartments, the average duration of infectiousness $(1/\gamma)$ is set equal to the average generation time (6.6 days) [4].

At each time t, the first dose is administered to a fraction $\alpha_{a,c}(t)$ of unvaccinated individuals in the population class {a,c}:

$$\alpha_{a,c}(t) = \frac{d_{a,c}(t)}{S_{a,c}(t) + I_{a,c}(t) + R_{a,c}(t)}$$

where $d_{a,c}(t)$ represents the number of (first) vaccine doses to be administered to individuals of the population class {a,c} at time t under the considered vaccination scenario. $d_{a,c}(t)$ is computed for each simulated scenario by taking into account vaccination priorities, coverage and capacity, and constraints on the expected supply of vaccine doses (details in Section 1.4).

We assume that the first dose becomes effective on average 14 days after administration, so $1/\omega_0 = 14$ days [11], that the second dose is administered 21 days after the first dose (i.e. $1/\omega_0 + 1/\omega_1 = 21$ days and $1/\omega_1 = 7$ days) [12], and that the 2nd dose becomes effective 7 days after administration, so $1/\omega_2 = 7$ days [11].

Vaccinated individuals $V_{i,a,c}$ (with i=0,1,2,3) can develop infection, but their susceptibility to infection is reduced by a factor $(1 - VE_{i,a})$, where $VE_{i,a}$ represents the age-specific vaccine efficacy associated to the *i-th* stage of protection. We assume that the vaccine efficacy is the same in individuals with and without comorbidities. In particular, to reflect the preferential administration of different vaccines to different age groups, we assume the efficacy associated to the AstraZeneca vaccine for the population under 55 years and that associated to Pfizer and Moderna for the over 55 (Table S1). Sensitivity analyses with respect to the assumed values were also performed (see Section 2.8).

Table S1. Age-specific vaccine efficacy in the different vaccination stages (baseline)

Parameters	Description	Age	
		0-54y	55y+
$VE_{0,age}$	Vaccine efficacy for vaccinated with the first dose, for whom the first dose is not effective yet ($V_{0,a,c}$)	0%	0%
$VE_{1,age}$	Vaccine efficacy for vaccinated with the first dose, for whom the first dose is effective ($V_{1,a,c}$)	76% [13]	80% [11,12,14]
$VE_{2,age}$	Vaccine efficacy for vaccinated with the second dose for whom the second dose is not effective yet ($V_{2,a,c}$)	76% [13]	80% [11,12,14]
$VE_{3,age}$	Vaccine efficacy for vaccinated with the second dose for whom the 2nd dose is effective.	81.3% [13]	95% [11,12,15]

1.2 Implementing perfect mitigation

The reproduction number associated to the dynamical system considered can be computed as the dominant eigenvalue of the Next Generation Matrix (NGM) [16,17,18], defined as:

$$(NGM)_{a,\tilde{a}} = \frac{\beta(1+\theta)\,(1-\varphi)\,\delta(t)}{\gamma} r_a C_{a,\tilde{a}} \Lambda_{\tilde{a}}(t) \qquad (1)$$

where $\Lambda_{\tilde{a}}(t)$ represents the fraction of individuals of age $\tilde{a}$ that are susceptible to SARS-CoV-2 at time t and is defined taking into account the reduced susceptibility in vaccinated compartments:

$$\Lambda_{\tilde{a}}(t) = \frac{\sum_c [S_{\tilde{a},c}(t) + (1-VE_{0,\tilde{a}})\,V_{0,\tilde{a},c}(t) + (1-VE_{1,\tilde{a}})V_{1,\tilde{a},c}(t) + (1-VE_{2,\tilde{a}})V_{2,\tilde{a},c}(t) + (1-VE_{3,\tilde{a}})V_{3,\tilde{a},c}(t)]}{N_{\tilde{a}}}$$

where $N_{\tilde{a}}$ represents the population of age $\tilde{a}$.

The distribution of the scaling factor shaping SARS-CoV-2 transmissibility for historical lineages (β) in the absence of PDRs ($\delta(t) = 1$) and other NPIs ($\varphi = 0$), can be computed analytically from Equation 1 given the distribution of the age-specific susceptibility profile (r_a), the distribution of the bootstrapped contact matrix $(C_{a,\tilde{a}})$, the value of γ and assuming $R_0 = 3$, as estimated in Italy in the early phase of the pandemic [4,5].

To implement the assumption of perfect mitigation, we use Equation 1 to recalibrate at each time step the value of $\delta(t)$ in order to obtain an approximately constant incidence, given the level of residual susceptibility in the population $\Lambda_{\tilde{a}}(t)$. When the value of $\delta(t)$ required to this purpose is higher than 1, we set its value to 1, corresponding to a complete reopening of society allowing pre-pandemic contacts to be fully resumed; in this case, the value of Rt will start declining, leading eventually to the suppression of transmission ("zero-COVID", i.e., no daily reported cases for at least two consecutive weeks).

Simulation results discussed in the main text and in the following sections were obtained by using a stochastic version of the model described above with a time step of 0.25 days. A total of 300 simulations were run for each scenario, sampling at each simulation a different value from the joint distribution of β, the bootstrapped contact matrices and the relative susceptibility in children.

1.3 Model initialization

The model population by age was initialized according to the Italian age structure in 2020 [19] and statistics on underlying conditions, including chronic respiratory disease, cardio-cerebrovascular disease, hypertension, diabetes and many others [20] (Figure S2).

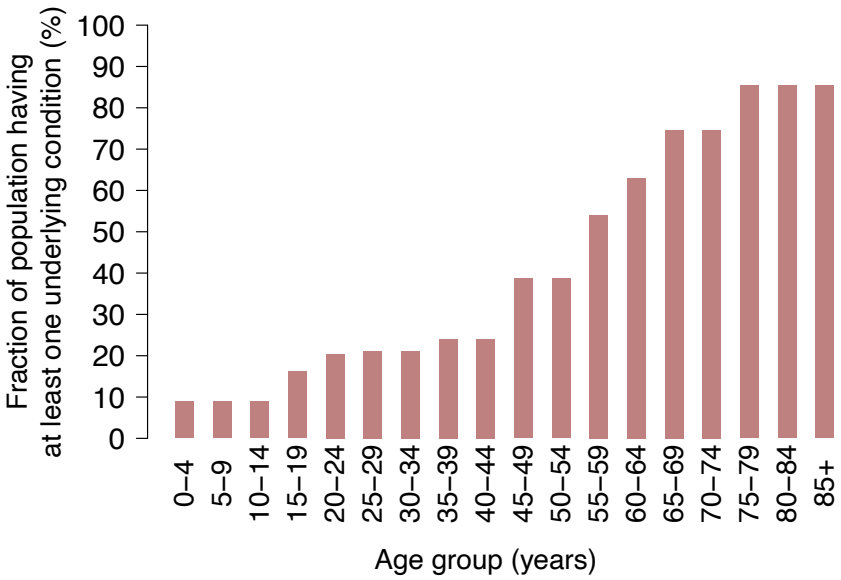

Figure S2. Fraction of the population having at least one underlying condition by age (%) [20]

<u>Fraction of initially immune individuals</u>. Estimates of the fraction of individuals recovered (and immune) from SARS-CoV-2 infection at the beginning of vaccination (end of December 2020) were obtained by re-calibrating a previously published model [21] until December 31 (Figure S3). In the baseline analysis we use the age-specific prevalence of SARS-CoV-2 estimated for the Lazio region, where about 16% of the overall population was estimated to have developed SARS-CoV-2 prior to the introduction of vaccination (Figure S3). Initially immune individuals were distributed homogeneously between individuals with and without underlying conditions. Different levels and age-distributions for the initial immunity were explored in a sensitivity analysis (see Section 2.11).

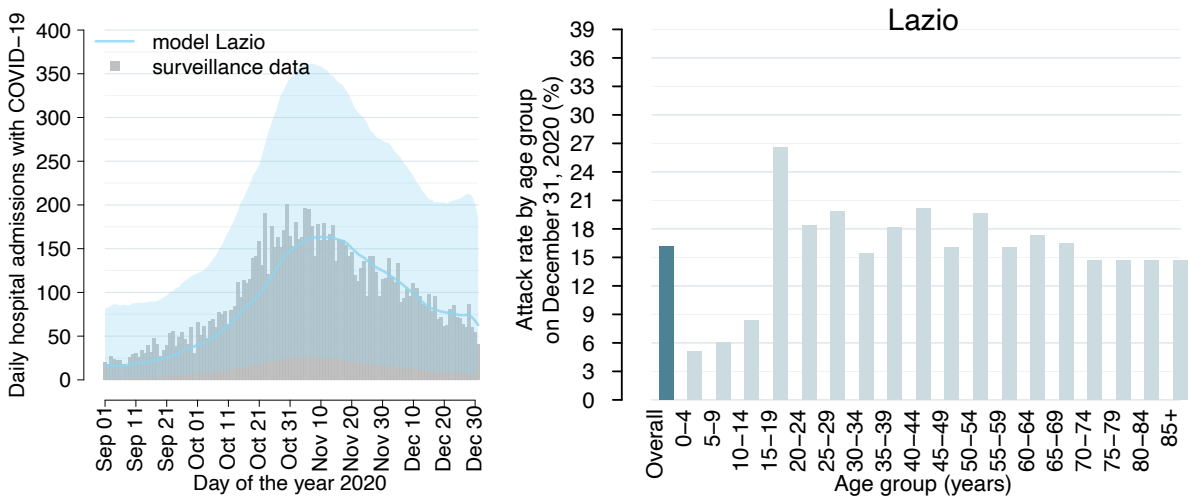

Figure S3. Estimated initial population immunity. Left: Daily hospitalizations with COVID-19 over time in the Lazio region, according to surveillance data [22] (gray bars) and as estimated by the model [21] (solid line, median; shaded area, 95% CI). Right: Overall and age-specific fraction of population infected with SARS-CoV-2 in the Lazio region at the beginning of the vaccination campaign (end of December 2020) [21].

Initially infectious individuals. The number of infected individuals at the beginning of simulations was determined in such a way to obtain, in the absence of vaccination, a weekly incidence of 50 reported cases per 100,000 population [23] (as a sensitivity analyses, we explore higher values of the incidence level: 100 weekly cases per 100,000; or 200 weekly cases per 100,000, see Section 2.7). The reporting rate ρ for SARS-CoV-2 infections at the end of 2020 was estimated as

$$\rho = \varepsilon / CFR$$

where ε is the infection fatality ratio estimated for Italy [24] and CFR is the case fatality ratio among SARS-CoV-2 cases reported in the last three weeks of December, assuming a delay between diagnosis and death of about 3 weeks [25]; thus, CFR=M/C where C is the cumulative number of cases reported in the last 3 weeks of December 2020 and M represents the number of deaths reported in the first 3 weeks of January 2021 [26]. The resulting value for the reporting rate is 37% (see Table S1).

1.4 Computation of age-specific vaccination rates over time

The delivery of vaccine doses is implemented by vaccinating a fixed number of individuals each day. The overall number of vaccine doses administered over time and by age depends on vaccine prioritization, daily vaccine administration capacity, vaccination coverage and on constraints on vaccine supply.

In the baseline analysis, we assumed a vaccination capacity of about 4 doses per 1,000 individuals (comparable with the influenza vaccination rates in the Italian population [27] and in line with other countries[28]). Different values of the daily vaccine administration capacity, i.e., 2, 6 or 8 doses per 1,000 individuals were explored as alternative scenarios (see Section 2.1).

The total number of available doses is distributed among the different population classes by considering different prioritizations. In the baseline analysis, we considered the order of priority suggested by the WHO SAGE roadmap [29], described in Table S2. The distribution of the population by age among the different priority tiers is shown in Figure S4. The age-specific vaccination coverage over time for the first dose, along with the timeline of vaccination of the different priority population is shown in Figure S5. Different priority orders are explored as sensitivity analyses (see Section 2.2). Vaccination in a given population segment is assumed to be complete when the vaccine uptake reaches a coverage of 75%, consistently with conservative estimates of vaccine acceptance [30,31,32]. Different coverage levels, i.e., 60% and 90%, are explored in alternative scenarios (see Section 2.3).

Table S2. Priority population of COVID-19 vaccination in the baseline analysis

Tier	Description	Counts (% of the population)
1	Health care workers	1,404,037[a] [33] (2.4%)
2	Residents in nursing homes	570,287[b] [33] (1.0%)
3	Over 80 years	3,993,128 (6.7%)
4	60-79y with at least one underlying condition	9,545,151 (16.0%)
5	<60 years with at least one underlying condition	10,797,835 (18.1%)
	60-79y without underlying conditions	3,459,503 (5.8%)
6	20-59 years (working age)	20,475,018 (34.3%)
7	Schoolchildren (5-19 y)	7,333,536 (12.3%)
8	Children under 5y	2,062,994 (3.4%)

[a]Age distribution of health care workers was obtained from [34]
[b]Age distribution of residents in nursing homes obtained from [35]

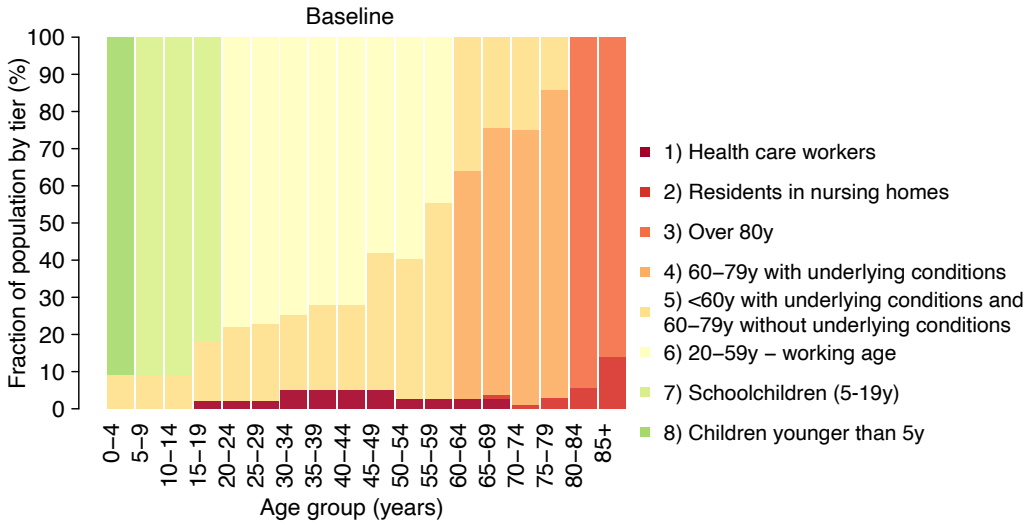

Figure S4. Population by priority tiers. Age-specific distribution of the population among the different priority tiers according to the order of priority considered in the baseline analysis.

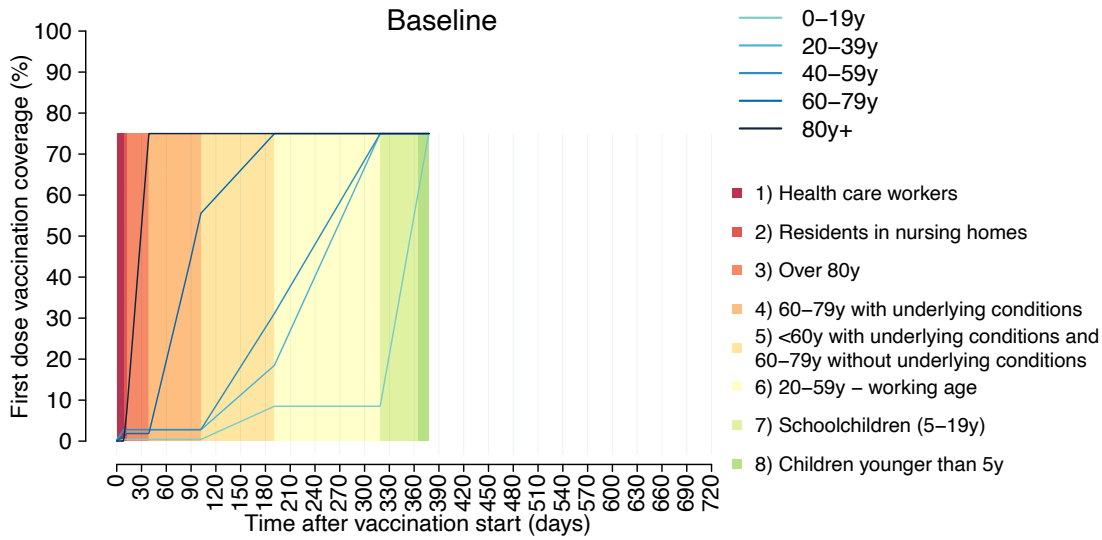

Figure S5. Deployment of the baseline vaccination campaign. First dose vaccination coverage in the different age groups (%). Colored areas denote the period in which the corresponding tier is targeted.

The daily vaccination supply was estimated from the number of vaccine doses expected to be delivered to Italy in each quarter of 2021 and in the first half of 2022 according to the preliminary agreements in early March 2021 [36]. We assume that the number of doses available in each quarter is distributed uniformly in the period. The effective number of vaccine doses that can be administered daily is computed as the minimum between the vaccine doses available and the vaccine administration capacity. If the vaccine supply in a quarter exceeds the total number of vaccine doses that the system is capable to administer, the doses in excess are cumulated to the vaccine supply of the following quarter. We assume that half of the doses administered are first doses, while the remaining half are second doses. Figure S6 shows a comparison between demand and supply of doses in the baseline scenario, showing that supply is expected to be a possible bottleneck for vaccine capacity only in the first quarter.

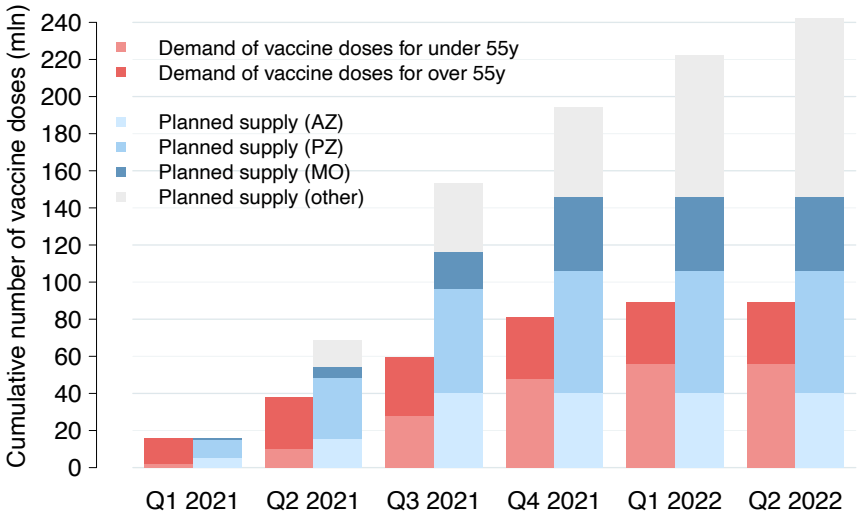

Figure S6. Comparison between vaccine demand in the baseline vaccination scenario and vaccine supplies as in the Italian plan for COVID-19 vaccination [36]

1.5 Model outputs

The main model outputs are the age-specific number of new infections per day in the subpopulation $i_{a,c}(t)$ and the scaling factor $\delta(t)$ tuning the proportion of pre-pandemic contacts that are allowed over the simulated period in order to have Rt=1 at all times. Each vaccination scenario is evaluated in terms of:

- cumulative incidence of SARS-CoV-2 deaths.
- percentage of relaxation of PDRs with respect to the pre-vaccination level required for mitigation in absence of a widespread circulation of hypertransmissible variants.

For each scenario, we report scatter plots of the cumulative incidence of deaths and the average PDR relaxation over the two years on individual simulations, to allow a first-glance comparison among scenarios and a more complete intuition of the bivariate dispersion of results.
We also report the median values and 95% confidence intervals across stochastic simulations of the percentage of PDRs relaxation and the potential reproduction number that would be observed if PDRs are completely relaxed at any given time.

<u>COVID-19 deaths.</u> We computed the daily number of deaths in each population class $D_{a,c}(t)$ by applying the age-specific infection fatality ratio estimated for each population class ($\varepsilon_{a,c}$) delayed by an average of 3 weeks (τ_D) between symptom onset and death [25]:

$$D_{a,c}(t) = \varepsilon_{a,c}\, i_{a,c}(t - \tau_D)$$

The age-specific IFR for each population class ($\varepsilon_{a,c}$) was estimated as:

$$\varepsilon_{a,c} = \psi_c \cdot \varepsilon_a = \nu \cdot \varepsilon_c \cdot \varepsilon_a$$

where

- ε_c denotes the overall IFR in class c, as estimated from Lombardy data [24].
- ε_a denotes the age-specific IFR as estimated independently of the presence of underlying conditions [24].
- the scale factor ν is determined in such a way to minimize the root mean square error between ε_a and $\tilde{\varepsilon}_a = \sum_c P_{a,c} \cdot \varepsilon_{a,c}$, and $P_{a,c}$ denotes the proportions of individuals of age a in class c in the Italian demographics [20].

Eventually, we obtain $\psi_{without}$=0.20 for individuals without underlying conditions and ψ_{with}=1.16 for individuals with underlying conditions, consistent with the overall relative risk $\frac{\psi_{with}}{\psi_{without}}$ = 5.8 [24].

Relaxation of PDRs. The percentage of PDRs relaxation at time t was computed with respect to restrictions required to maintain Rt=1 at the beginning of vaccination (δ^*). Since at the beginning of vaccination more transmissible lineages were not widespread, δ^* is defined as the value of $\delta(t)$ obtained at the beginning of simulations when assuming no increase in transmissibility with respect to historical lineages (i.e. $\theta = 0\%$). The relaxation of PDRs was thus computed as:

$$P_{relax}(t) = \frac{\delta(t) - \delta^*}{(1 - \delta^*)} \cdot 100$$

Potential reproduction number. For each scenario and for each time t the potential reproduction number is computed as the dominant eigenvalue of the Next Generation Matrix defined in Equation (1) by setting $\delta(t) = 1$, to account for complete relaxation of PDRs, i.e.:

$$(\mathrm{NGM})_{a,\tilde{a}} = \frac{\beta(1+\theta)(1-\varphi)}{\gamma} \mathrm{r_a C_{a,\tilde{a}} \Lambda_{\tilde{a}}}\,(t)$$

When the potential reproduction number falls below the epidemic threshold of 1, the accumulated immunity will be sufficient to avoid a resurgence of widespread transmission (although local outbreaks due to the heterogeneity of immunity across the population are always possible).

2. Sensitivity analyses

We run a number of analyses with different assumptions in parameter values and model structure, which are described in detail in this section. Table S3 summarizes the main model parameters and assumptions in the baseline and in alternative sensitivity analyses.

Table S3. Description of key parameters and assumption used in the model and in alternative scenarios

Parameter description	Baseline	Alternative
Epidemiological		
Generation time ($1/\gamma$)	6.6 days [4]	-
Age-specific susceptibility to infection (r_a)	$r_a = 0.58$ (95%CI 0.34-0.98) for $a < 15$ years; $r_a = 1$ for $15 \leq a < 65$ years; $r_a = 1.65$ (95%CI 1.03-2.65) when $a \geq 65$ years [3]	r_a=1 for all ages (homogeneous susceptibility)
Duration of immunity after SARS-CoV-2 infection	Long-lived (at least 2 years)	-
Age-group specific contact matrix ($C_{a,\tilde{a}}$)	Contact matrix estimated for Italy [1,2]	-
Maximum relaxation of PDRs allowed	100%	• 0%
Initially immune individuals by age	medium scenario (average population immunity: ~16%)	• low immunity scenario (~9%) • high immunity scenario (~23%)
SARS-CoV-2 reporting ratio (ρ)	37.3%	-
Target incidence of SARS-CoV-2 reported cases for mitigation	50 cases per 100,000 population per week [23]	• 100 per 100,000 • 200 per 100,000
Vaccination		
Vaccine protection	Infection	Disease
Number of doses	2	-
Target population	All individuals, independently from a previous diagnosis of COVID-19	-
Delay between 1st dose and achievement of vaccine efficacy	14 days [11]	-
Interval between 1st and 2nd dose	21 days [12]	-
Delay between 2nd dose and achievement of vaccine efficacy	7 days [11]	-
Efficacy immediately after 1st dose ($VE_{0,a}$)	0% for all ages	-
Full efficacy of 1st dose ($VE_{1,a}$)	• 76% for $a < 55$ years [13] • 80% for $a \geq 55$ years [11,12,14]	• 15% lower than the baseline • 0% for all ages
Efficacy immediately after 2nd dose ($VE_{2,a}$)	Same as $VE_{1,a}$	Same as $VE_{1,a}$
Full efficacy of 2nd dose ($VE_{3,a}$)	• 81.3% for $a < 55$ years [13] • 95% for $a \geq 55$ years [11 ,12, 15]	• 15% lower than the baseline
Vaccination capacity (maximum number of daily doses administered)	4 per 1,000 population (details in Supplementary Material 1)	• 2 per 1,000 population • 6 per 1,000 population • 8 per 1,000 population
Vaccine coverage	75% for all ages	• 60% • 90%
Duration of vaccine protection	Long-lived (at least 2 years)	• 6 months • 1 year • 18 months • 2 years
Priority population	1. Health care workers (HCW) 2. Patients in nursing homes 3. Over 80 years 4. 60-79 years with underlying conditions 5. <60 years with underlying conditions; 60-79 years without underlying conditions 6. 20-59 years (working age) 7. Schoolchildren (5-19 years) 8. Children under 5 years of age	After HCW and patients in nursing homes: • "Elderly": priority based on age (independently of comorbidities) • "Working age": working age groups (20-59y), then elderly (60+), then children (0-19y). • "Schoolchildren": schoolchildren (5-19y); then working age groups (20-59y), then elderly (60+), then pre-school children <5y

2.1 Vaccination capacity

We explored different values for the daily vaccination administration capacity: 2, 6 or 8 doses per 1,000 individuals. The priority order considered in these additional analyses (Table S2 and Figure S5) and the vaccination coverage (75%) are the same as in the baseline. The age-specific first-dose vaccination coverage over time, along with the timeline of vaccination of the different priority populations under the different vaccination capacities considered are shown in Figures S7-S9.

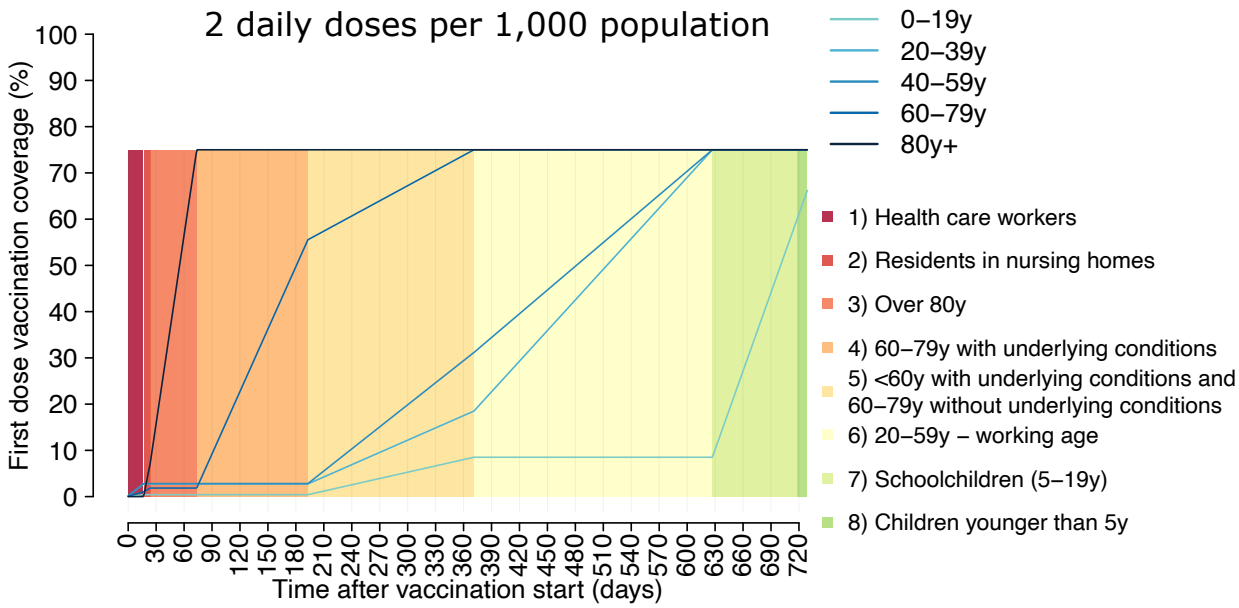

Figure S7. Deployment of the vaccination campaign under a daily vaccination capacity of 2 doses per 1,000 population. First dose vaccination coverage in the different age groups (%). Colored areas denote the period in which the corresponding priority tier is targeted.

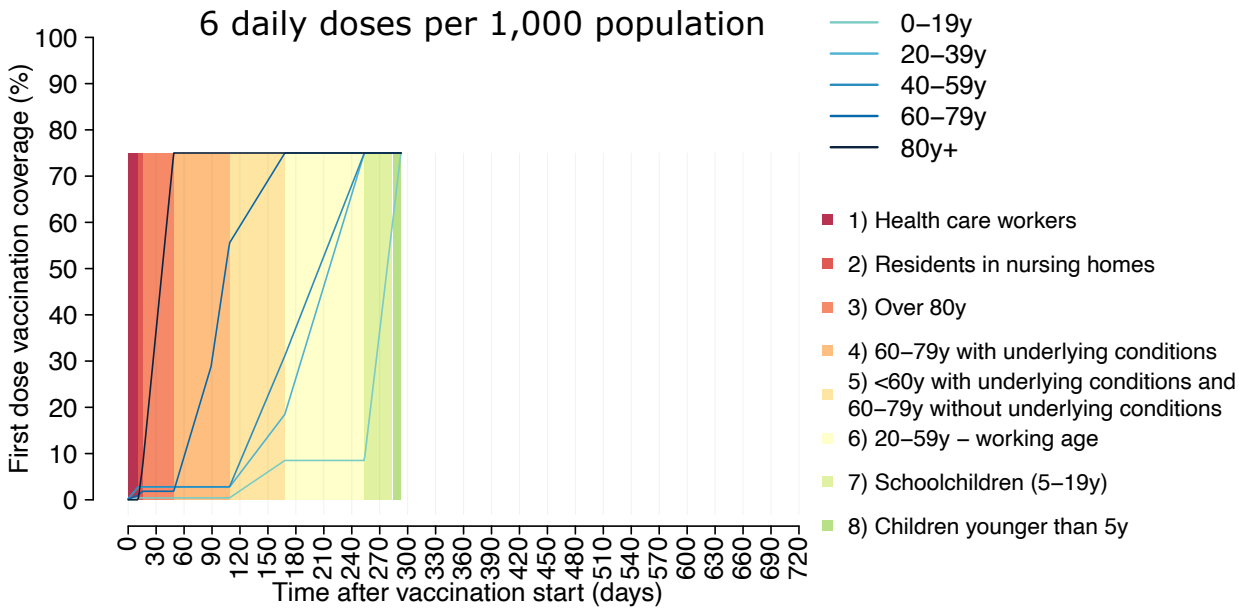

Figure S8. Deployment of the vaccination campaign under a daily vaccination capacity of 6 doses per 1,000 population. First dose vaccination coverage in the different age groups (%). Colored areas denote the period in which the corresponding priority tier is targeted.

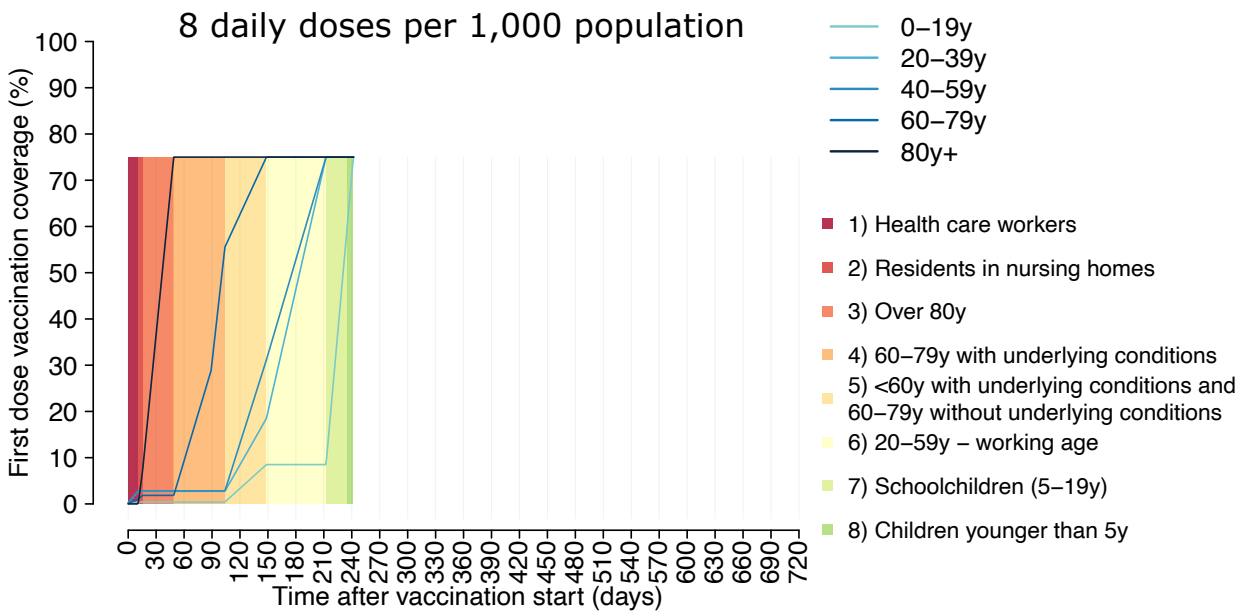

Figure S9. Deployment of the vaccination campaign under a daily vaccination capacity of 8 doses per 1,000 population. First dose vaccination coverage in the different age groups (%). Colored areas denote the period in which the corresponding priority tier is targeted.

2.2 Priority population

We explored alternative prioritization orders for vaccination. In all sensitivity analyses on priority population, we fixed healthcare workers and nursing home residents in priority tier 1 and 2. The remaining population is vaccinated as described in Table S4 by considering different orders of prioritization only based on age and disregarding the presence of underlying conditions. In particular, we focused on four alternative strategies:

- "Elderly" denotes a strategy in which age represents the unique determinant of priority, independently from the presence of underlying conditions.
- "Working age" denotes a strategy which aims at immunizing the active population age-segments first (working age), followed by older population age segments, then by schoolchildren and pre-schoolchildren.
- "Schoolchildren" denotes a strategy which aims at immunizing high-transmission population segments first, i.e. individuals with higher social mixing. Under this strategy, we assume to vaccinate school-age children (characterized by the highest contact rates) first, followed by working-age adults and then by older population age segments (at higher risk of severe outcome of COVID-19).
- "Children under 15y excluded from vaccination". In this strategy we assume that available vaccines will not be licensed for children under 15 years of age. Prioritization order for the rest of population is the same as in the baseline.

The age-specific first-dose vaccination coverage over time, along with the timeline of vaccination under the different priority populations considered are shown in Figure S10-S13. Results obtained for the alternative prioritization strategies are presented in Figure S14.

Table S4. Priority population of COVID-19 vaccination in the sensitivity analyses

Sensitivity analysis "Elderly"		
Tier	Description	Counts (% of the population)
1	Health care workers	1,404,037[a] [33] (2.4%)
2	Residents in nursing homes	570,287[b] [33] (1.0%)
3	Over 80y	3,993,128 (6.7%)
4	60-79y	13,004,654 (21.8%)
5	20-59 y (working age)	30,129,505 (50.5%)
6	Schoolchildren (5-19 y)	8,275,340 (13.9%)
7	Children under 5y	2,264,538 (3.8%)
Sensitivity analysis "Working age"		
Tier	Description	Counts (% of the population)
1	Health care workers	1,404,037[a] [33] (2.4%)
2	Residents in nursing homes	570,287[b] [33] (1.0%)
3	20-59 y (working age)	30,129,505 (50.5%)
4	60-79y	13,004,654 (21.8%)
5	Over 80 y	3,993,128 (6.7%)
6	Schoolchildren (5-19 y)	8,275,340 (13.9%)
7	Children under 5y	2,264,538 (3.8%)
Sensitivity analysis "School age"		
Tier	Description	Counts (% of the population)
1	Health care workers	1,404,037[a] [33] (2.4%)
2	Residents in nursing homes	570,287[b] [33] (1.0%)
3	Schoolchildren (5-19 y)	8,275,340 (13.9%)
4	20-59 (working age)	30,129,505 (50.5%)
5	60-79y	13,004,654 (21.8%)
6	Over 80 y	3,993,128 (6.7%)
7	Children under 5y	2,264,538 (3.8%)
Sensitivity analysis "Children under 15y excluded from vaccination"		
Tier	**Description**	**Counts (% of the population)**
1	Health care workers	1,404,037[a] [33] (2.4%)
2	Residents in nursing homes	570,287[b] [33] (1.0%)
3	Over 80 years	3,993,128 (6.7%)
4	60-79y with at least one underlying condition	9,545,151 (16.0%)
5	<60 years with at least one underlying condition	10,797,835 (18.1%)
	60-79y without underlying conditions	3,459,503 (5.8%)
6	20-59 years (working age)	20,475,018 (34.3%)
7	Schoolchildren (15-19 y)	2,356,728 (4.0%)

[a]Age distribution of health care workers was obtained from [34]
[b]Age distribution of residents in nursing homes obtained from [35]

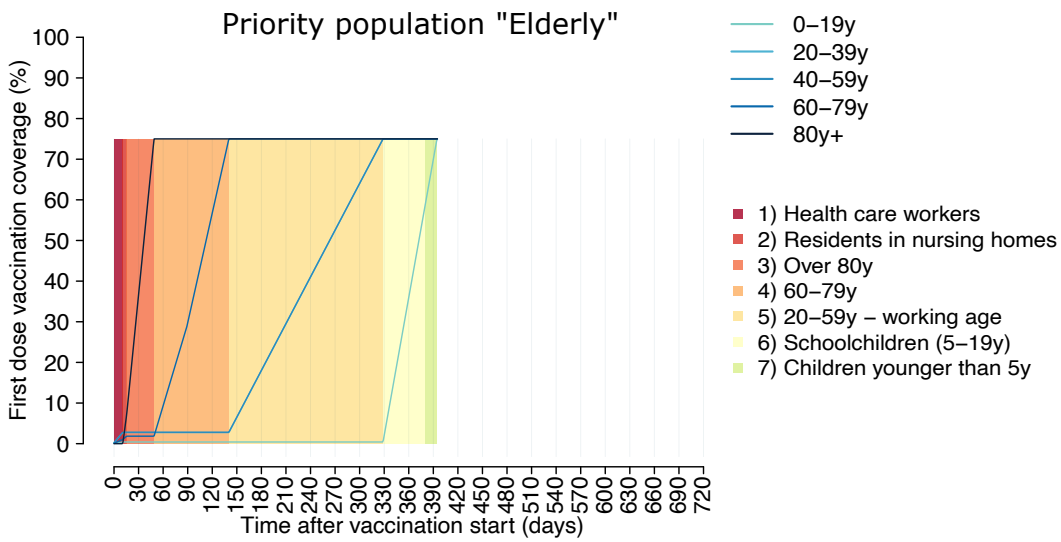

Figure S10. Deployment of the vaccination campaign under the "Elderly" prioritization strategy. First dose vaccination coverage in the different age groups (%). Colored areas denote the period in which the corresponding tier is targeted.

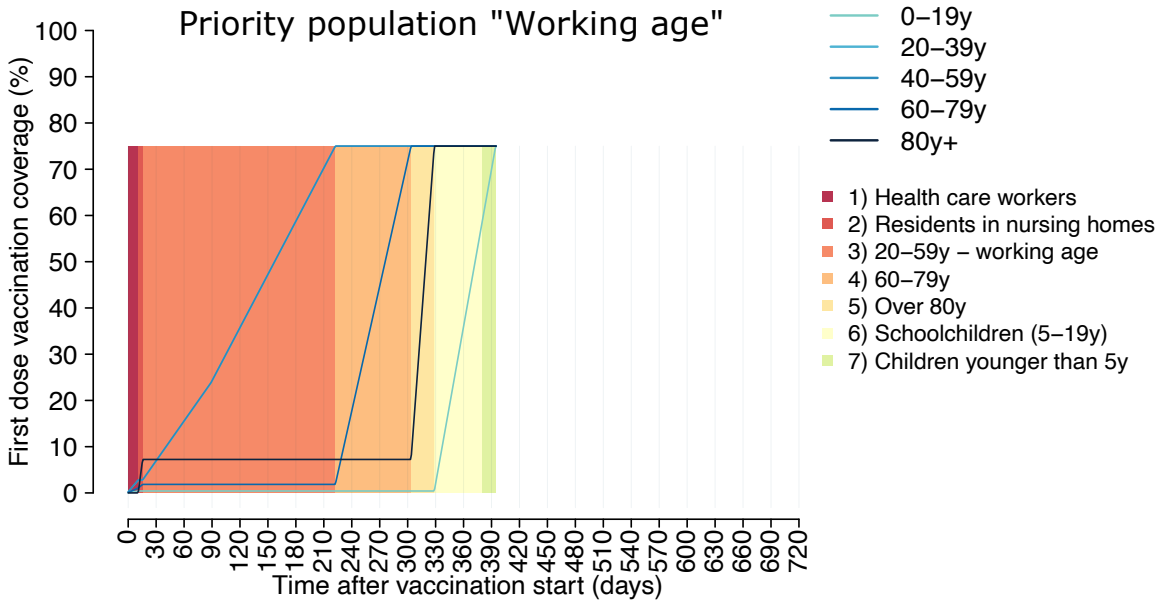

Figure S11. Deployment of the vaccination campaign under the "Working age" prioritization strategy. First dose vaccination coverage in the different age groups (%). Colored areas denote the period in which the corresponding tier is targeted.

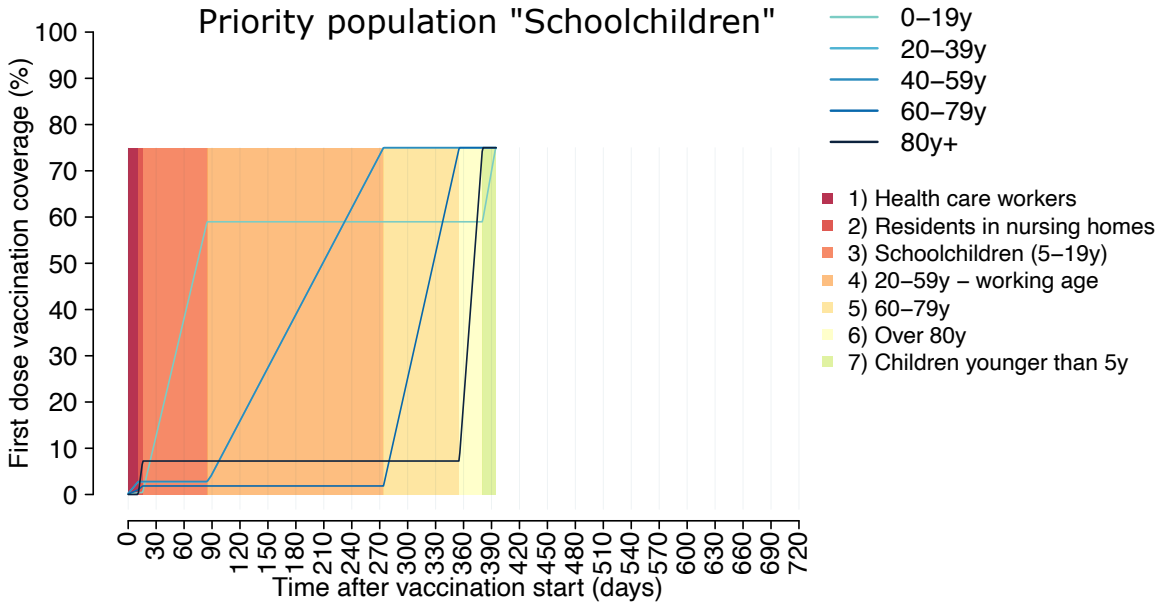

Figure S12. Deployment of the vaccination campaign under the "School age" prioritization strategy. First dose vaccination coverage in the different age groups (%). Colored areas denote the period in which the corresponding tier is targeted.

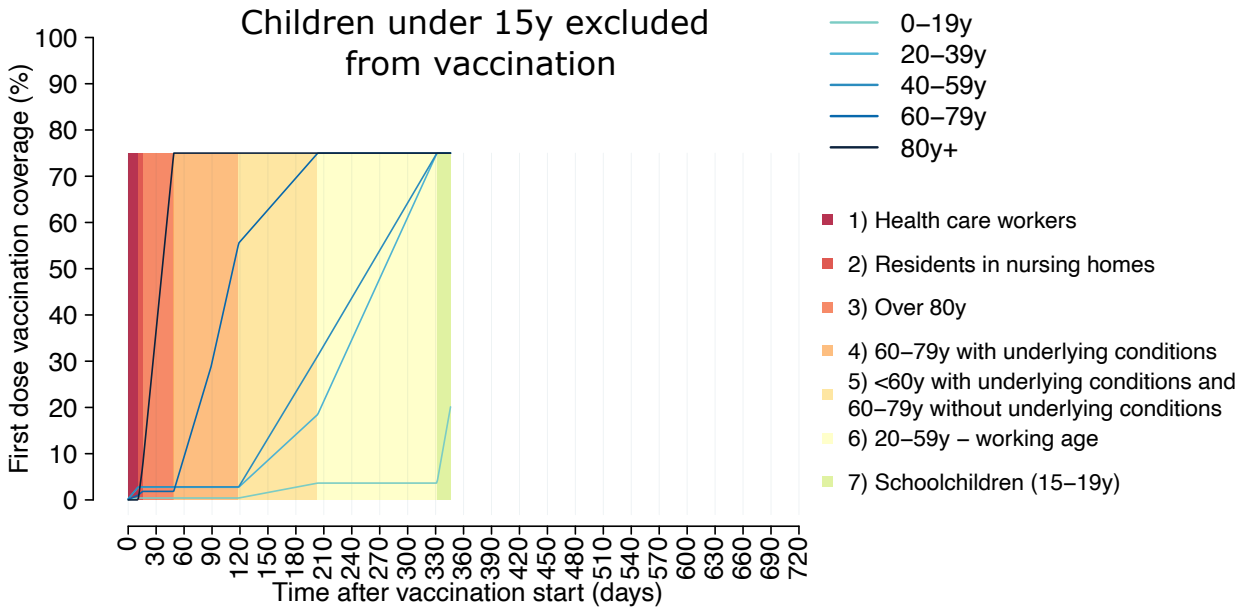

Figure S13. Deployment of the vaccination campaign when assuming that children under 15y are not eligible for vaccination. First dose vaccination coverage in the different age groups (%). Colored areas denote the period in which the corresponding tier is targeted.

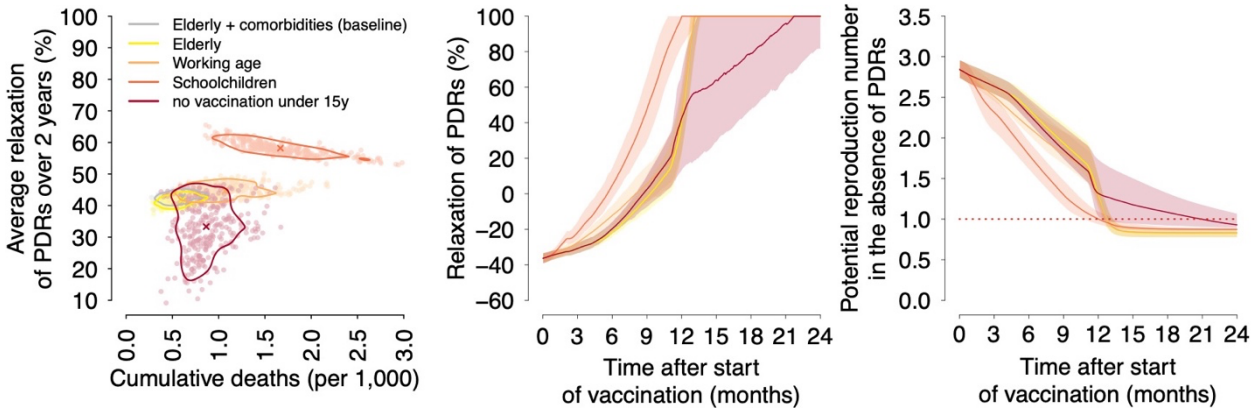

Figure S14. Alternative prioritization strategies. Left: comparison between scenarios in terms of the cumulative incidence of deaths and the average relaxation of PDRs over the two simulated years. Individual stochastic simulations are shown as points, the mean of their bivariate distribution as crosses and its 75-percentile as closed curves. Center: relaxation of PDRs over time. Solid lines indicate the median, shaded areas the 95% projection interval. Right: potential reproduction number over time. Solid lines indicate the median, shaded areas the 95% projection interval. The horizontal dashed red line indicates the epidemic threshold.

2.3 Vaccine coverage

We explored lower/higher vaccination coverage values (60% or 90%) compared to the baseline. The daily vaccination capacity and the priority order considered in these additional analyses were the same as the baseline (4 daily doses per 1,000 population and priority specified in Table S2).

The age-specific first-dose vaccination coverage over time, along with the timeline of vaccination under the alternative coverage levels considered are shown in Figures S15-S16.

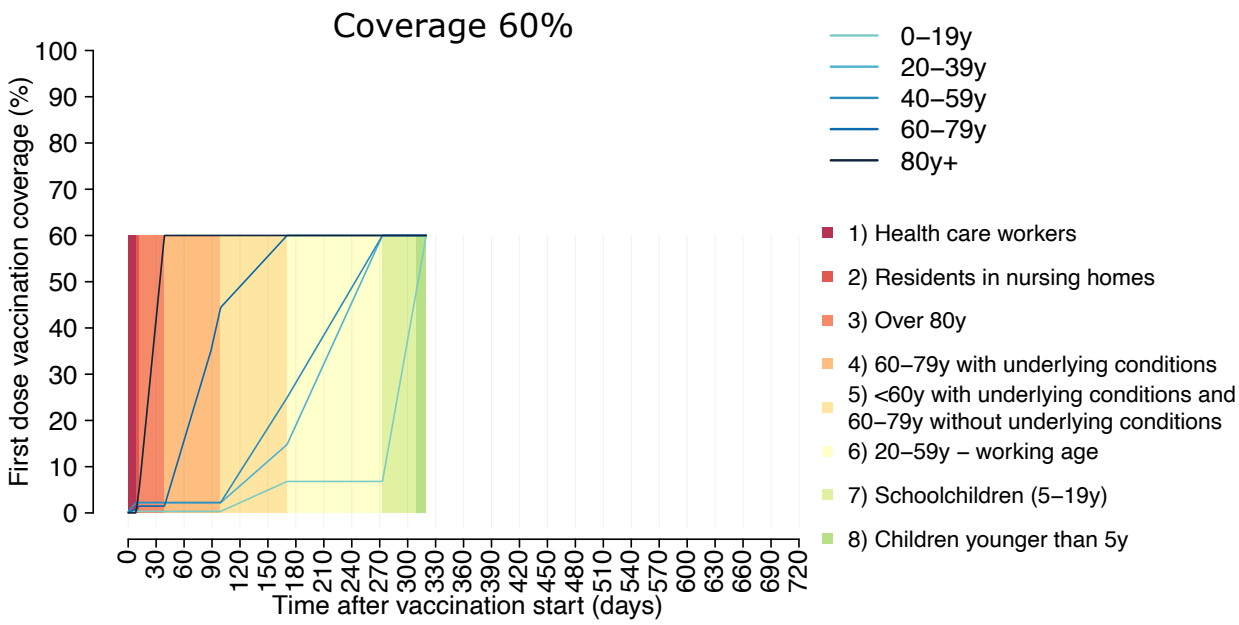

Figure S15. Deployment of the vaccination campaign assuming a 60% vaccination coverage. First dose vaccination coverage in the different age groups (%). Colored areas denote the period in which the corresponding tier is targeted.

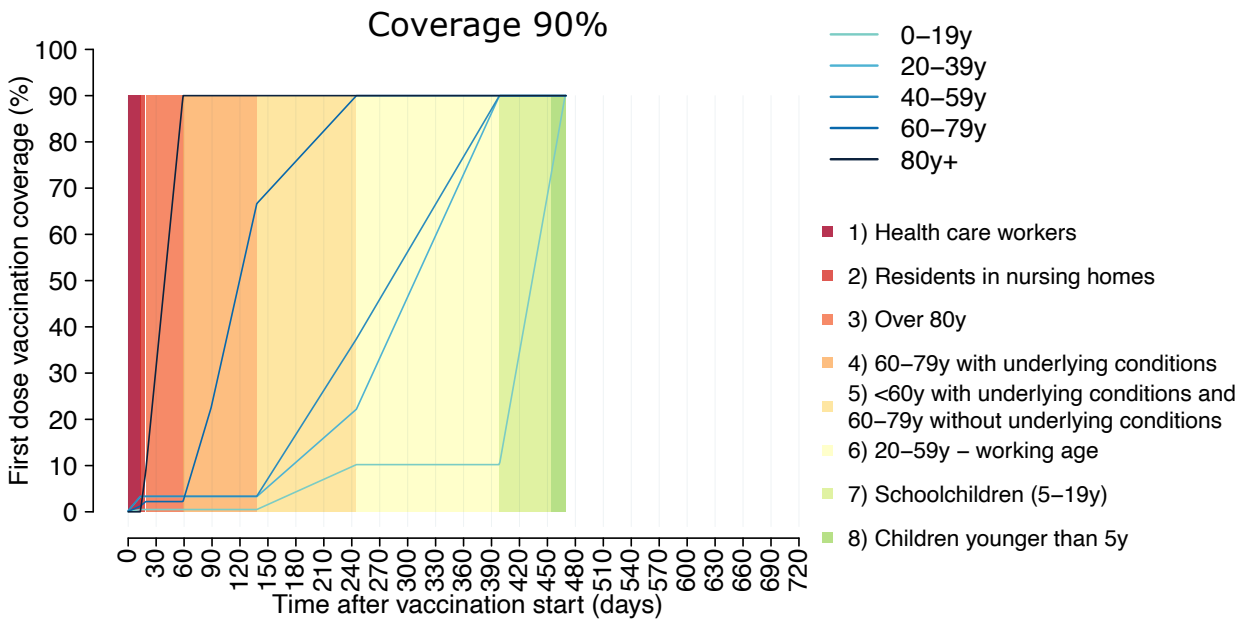

Figure S16. Deployment of the vaccination campaign assuming a 90% vaccination coverage. First dose vaccination coverage in the different age groups (%). Colored areas denote the period in which the corresponding tier is targeted.

2.4 Duration of vaccine protection

The model used to run sensitivity analyses with shorter duration of vaccine-induced protection is summarized in Figure S17. The model has the same structure, parameters and epidemiological compartments of the baseline model except for an additional compartment W, denoting individuals vaccinated with two doses for whom vaccine protection has waned. After waning of vaccine-induced protection individuals have the same susceptibility to SARS-CoV-2 infection of unvaccinated individuals. In this sensitivity analysis we explore average durations of vaccine-induced protection $(1/\omega_3)$ of 6 months, 1 year, 18 months and 2 years.

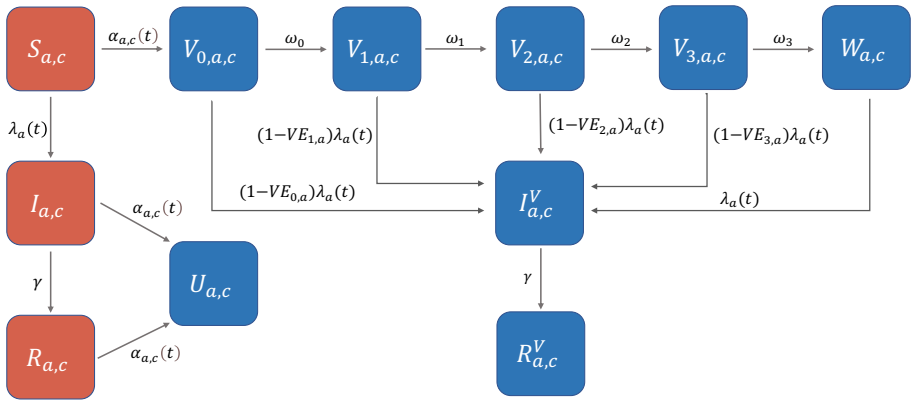

Figure S17. Schematic representation of the model including waning of vaccine protection. Red compartments represent unvaccinated individuals and therefore eligible for vaccination; blue compartments represent vaccinated individuals. Model parameters include: the time- and age-dependent force of infection $\lambda_a(t)$; the recovery rate from infection (γ); the time-, age- and group-dependent probability of being vaccinated $\alpha_{a,c}(t)$; the interval between administration of the first dose and full protection by the first dose ($1/\omega_0$); the interval between full protection of the first dose and administration of the second dose ($1/\omega_1$); the interval between administration of the second dose and full protection of the 2nd dose ($1/\omega_2$); the interval between full protection of the second dose and waning of vaccine protection ($1/\omega_3$); age-dependent vaccine efficacies in the different stages *i* of vaccine protection (i=0,1,2,3) are denoted by $VE_{i,a}$.

2.5 Increased mortality

Given the uncertainty surrounding estimates of the relative transmissibility of B.1.1.7 with respect to historical lineages, we explore lower/higher values for the coefficient θ ={30%, 70%}.

In addition, we also tested the effect of an increased mortality of infections, which has been ascertained for at least one variant lineage [37,38], under the baseline assumption on the relative transmissibility (θ =50%). We implement this as a scaling factor k on the IFR for all age classes:

$$\varepsilon^{inc}_{a,c} = k\varepsilon_{a,c}$$

where k=1.64 [37,38].

Results obtained for this scenario are shown in Figure S18.

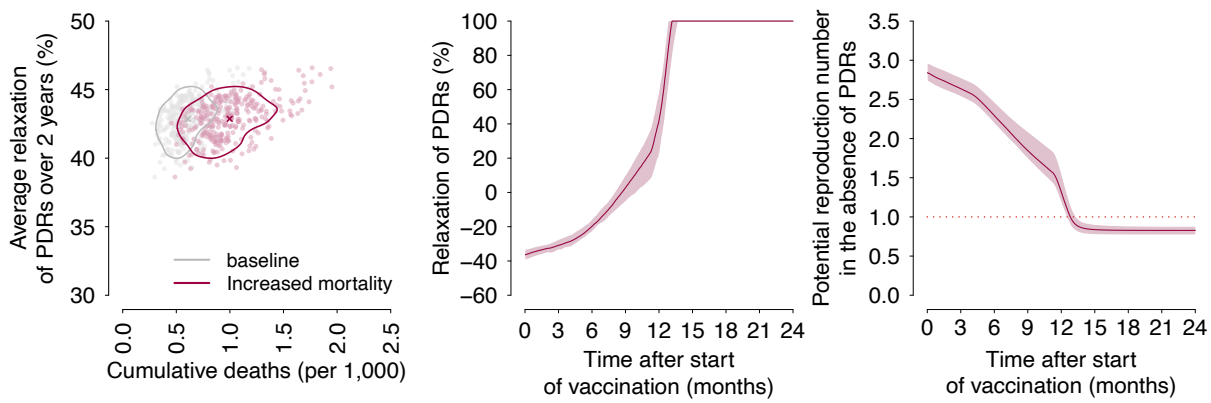

2.6 **Figure S18. Increased mortality.** Left: comparison between scenarios in terms of the cumulative incidence of deaths and the average relaxation of PDRs over the two simulated years. Individual stochastic simulations are shown as points, the mean of their bivariate distribution as crosses and its 75-percentile as closed curves. Center: relaxation of PDRs over time. Solid lines indicate the median, shaded areas the 95% projection interval. Right: potential reproduction number over time. Solid lines indicate the median, shaded areas the 95% projection interval. The horizontal dashed red line indicates the epidemic threshold.

2.6 Complete reopening after vaccination of the most fragile

In this scenario, we rescale the value of $\delta(t)$ (corresponding to maintain mitigation measures) only until all individuals with underlying conditions or of age above 60 years have been vaccinated, after which $\delta(t)$ is set to 1 until the end of simulations (corresponding to a complete reopening of society).

2.7 Incidence level of reported cases

We explored incidence levels admitted by mitigation measures that are higher than the baseline, namely 100 or 200 weekly reported cases per 100,000 population. All other parameters, including coverage, capacity and priority populations are the same as the baseline analysis.

Results obtained, summarized in Figure S19, suggest that higher incidence levels accelerate the relaxation of PDRs, due to the increased accumulation of immunity associated to a more sustained circulation of SARS-CoV-2. However, these sensitivity analyses result in a two- to four-fold increase in the cumulative number of deaths.

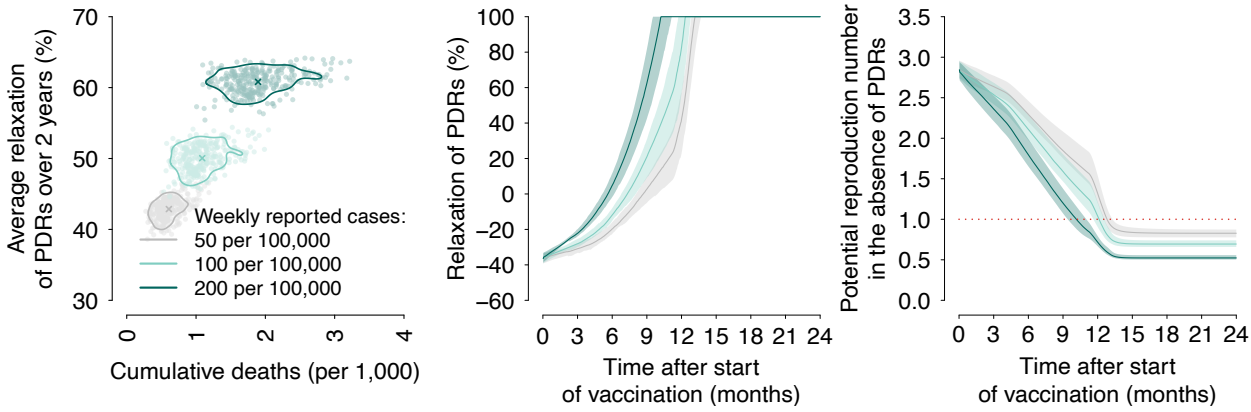

Figure S19. Alternative incidence level scenarios. Left: comparison between scenarios in terms of the cumulative incidence of deaths and the average relaxation of PDRs over the two simulated years. Individual stochastic simulations are shown as points, the mean of their bivariate distribution as crosses and its 75-percentile as closed curves. Center: relaxation of PDRs over time. Solid lines indicate the median, shaded areas the 95% projection interval. Right: potential reproduction number over time. Solid lines indicate the median, shaded areas the 95% projection interval. The horizontal dashed red line indicates the epidemic threshold.

2.8 Vaccine efficacy

We explored alternative values for the vaccine efficacy in the different vaccination stages. First, we consider a vaccine for which the first dose alone does not provide any protection against infection (Table S5). Second, we consider a vaccine with efficacy reduced by about 15% compared to the baseline for all ages and in all vaccination stages (Table S6). All other parameters, including coverage, capacity and priority population are the same as the baseline analysis. As shown in Figure S20, the vaccine efficacy after the first dose affects only marginally results obtained, both in terms of cumulative deaths and percentage of PDRs relaxation. A reduced vaccine efficacy after the second dose results in a death burden that is about 40% higher.

Table S5. Vaccine efficacy in the different vaccination stages (sensitivity "0% after the first dose")

Parameters	Description	Age	
		0-54y	55y+
$VE_{0,age}$	Vaccine efficacy for vaccinated with the first dose, for whom the first dose is not effective yet ($V_{0,a,c}$)	0%	0%
$VE_{1,age}$	Vaccine efficacy for vaccinated with the first dose, for whom the first dose is effective ($V_{1,a,c}$)	0%	0%
$VE_{2,age}$	Vaccine efficacy for vaccinated with the second dose for whom the second dose is not effective yet ($V_{2,a,c}$)	0%	0%
$VE_{3,age}$	Vaccine efficacy for vaccinated with the second dose for whom the 2nd dose is effective.	81.3% [13]	95% [11,12,15]

Table S6. Vaccine efficacy in the different vaccination stages (sensitivity "reduced for both doses")

Parameters	Description	Age	
		0-54y	55y+
$VE_{0,age}$	Vaccine efficacy for vaccinated with the first dose, for whom the first dose is not effective yet ($V_{0,a,c}$)	0%	0%
$VE_{1,age}$	Vaccine efficacy for vaccinated with the first dose, for whom the first dose is effective ($V_{1,a,c}$)	64%	67%

$VE_{2,age}$	Vaccine efficacy for vaccinated with the second dose for whom the second dose is not effective yet ($V_{2,a,c}$)	64%	67%
$VE_{3,age}$	Vaccine efficacy for vaccinated with the second dose for whom the 2nd dose is effective.	68%	80%

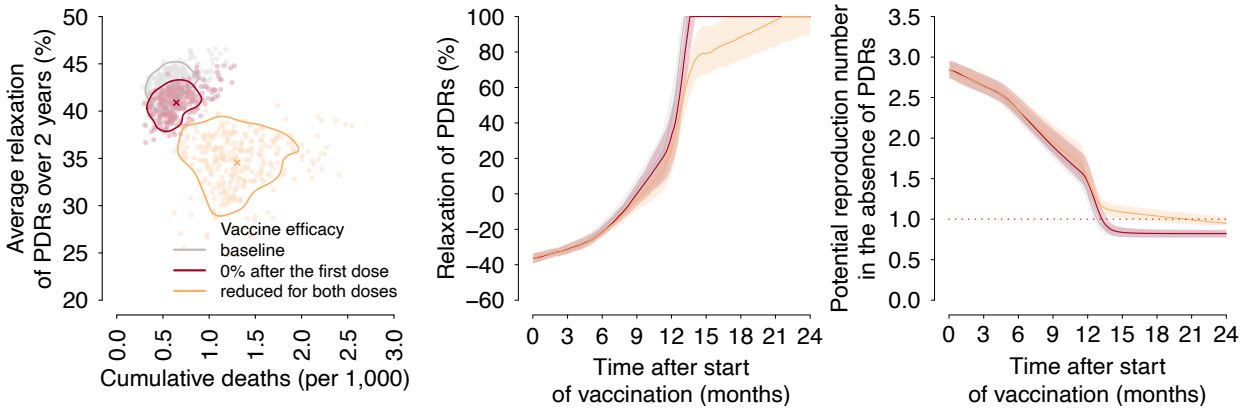

Figure S20. Alternative vaccine efficacy scenarios. Left: comparison between scenarios in terms of the cumulative incidence of deaths and the average relaxation of PDRs over the two simulated years. Individual stochastic simulations are shown as points, the mean of their bivariate distribution as crosses and its 75-percentile as closed curves. Center: relaxation of PDRs over time. Solid lines indicate the median, shaded areas the 95% projection interval. Right: potential reproduction number over time. Solid lines indicate the median, shaded areas the 95% projection interval. The horizontal dashed red line indicates the epidemic threshold.

2.9 Homogeneous susceptibility

We evaluated the model sensitivity to the assumption that susceptibility to infectious is reduced in children and increased in older adults; while this is now an acquired fact for historical lineages [3, 39], it may not be necessarily so for variants. Under the assumption of a susceptibility that remains equal in all age classes, we recalibrated the value of β and applied all other conditions as in the baseline scenario. We project a slightly delayed reopening, but a considerably smaller number of deaths (Figure S21).

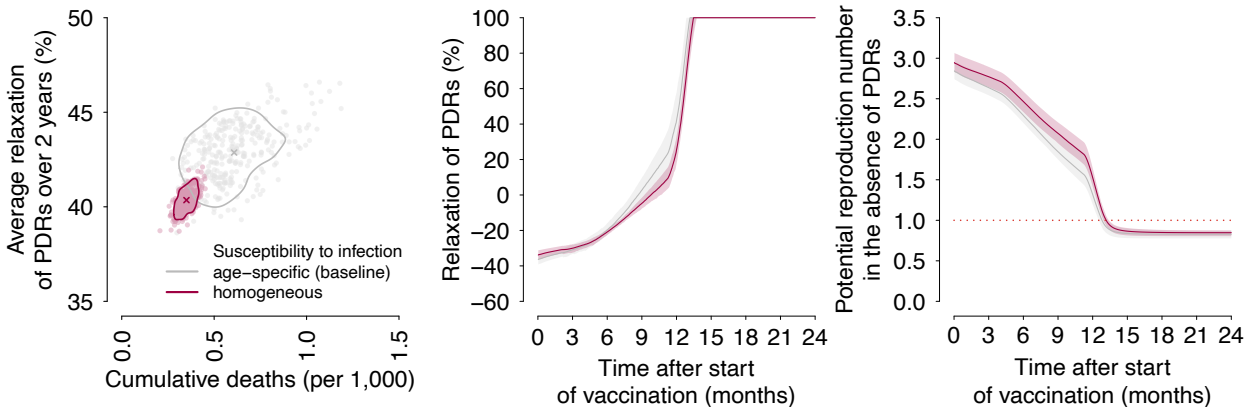

Figure S21. Homogeneous susceptibility. Left: comparison between scenarios in terms of the cumulative incidence of deaths and the average relaxation of PDRs over the two simulated years. Individual stochastic simulations are shown as points, the mean of their bivariate distribution as crosses and its 75-percentile as closed curves. Center: relaxation of PDRs over time. Solid lines indicate the median, shaded areas the 95% projection interval. Right: potential reproduction number over time. Solid lines indicate the median, shaded areas the 95% projection interval. The horizontal dashed red line indicates the epidemic threshold.

2.10 Vaccine protection

We adapted the model to evaluate a sensitivity analysis where a vaccine provides protection against disease, but not infection (Figure S22). Differently from the baseline model, vaccination does not reduce susceptibility to SARS-CoV-2 infection. Indeed, the force of infection to which vaccinated individuals are exposed is the same as unvaccinated individuals. However, in this analysis infections occurring among vaccinated individuals are characterized by a reduced probability of death compared to unvaccinated ones.

In this case, the daily number of deaths $\mathrm{D_{a,c}(t)}$ is computed as follows:

$$\mathrm{D_{a,c}(t)} = \varepsilon_{\mathrm{a,c}} i^{S}_{a,c}(\mathrm{t}-\tau_{\mathrm{D}}) + \sum_{j=0}^{3}(1-\mathrm{VE}_{j,\mathrm{a}})\varepsilon_{\mathrm{a,c}} i^{V_j}_{a,c}(\mathrm{t}-\tau_{\mathrm{D}})$$

where

- $i^{S}_{a,c}(t)$ represents the age-specific number of new infections among unvaccinated individuals per day in the subpopulation *c*
- $i^{V_j}_{a,c}(t)$ represent the age-specific numbers of new infections among individuals in the j-th vaccination stage per day in the subpopulation *c*
- $\varepsilon_{\mathrm{a,c}}$ is the age-specific infection fatality ratio [24]
- $\mathrm{VE}_{j,\mathrm{a}}$represents the age-specific vaccine efficacy in the *j*-th vaccination stage
- τ_{D} represents the time between symptom onset and death [25]

Results obtained are shown in Figure S23. A vaccine protecting against disease would allow a very limited relaxation of PDRs (namely, the same expected in the absence of vaccination), but the overall number of deaths would be greatly reduced compared to a no vaccination scenario, although still about 70% higher than the baseline scenario.

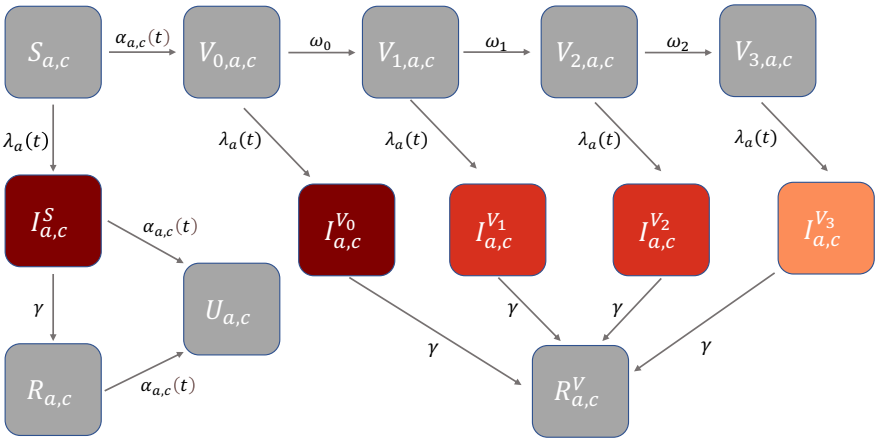

Figure S22. Schematic representation of the model of a vaccine providing protection against disease but not infection. The model has the same structure and parameters as the baseline model, except that vaccinated individuals are subject to the same force of infection λ as unvaccinated ones, and that the corresponding infectious stages are kept distinct to allow a computation of the number of resulting deaths taking into account the stage-specific vaccine protection.

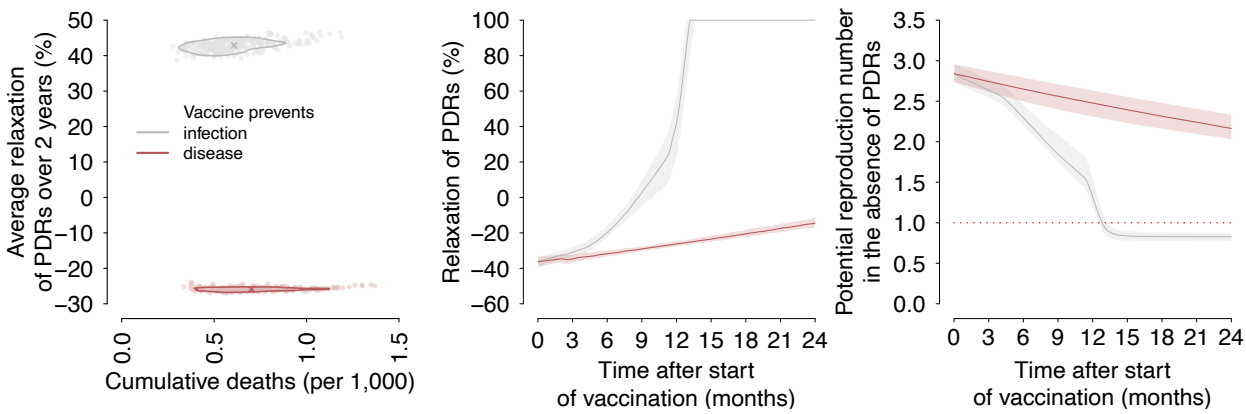

Figure S23. Vaccine providing protection against disease. Left: comparison between scenarios in terms of the cumulative incidence of deaths and the average relaxation of PDRs over the two simulated years. Individual stochastic simulations are shown as points, the mean of their bivariate distribution as crosses and its 75-percentile as closed curves. Center: relaxation of PDRs over time. Solid lines indicate the median, shaded areas the 95% projection interval. Right: potential reproduction number over time. Solid lines indicate the median, shaded areas the 95% projection interval. The horizontal dashed red line indicates the epidemic threshold.

2.11 Initial immunity

We assessed the robustness of our conclusions with respect to different levels of initial immunity in the population (lower or higher than the baseline). We used estimates of the fraction of individuals recovered from SARS-CoV-2 infection at the beginning of vaccination (end of December 2020) obtained by re-calibrating a previously published model [21] until December 31 in the Campania region and in the Lombardy region (Figure S24 and S25).

In the scenario with lower immunity, we initialized the population according to the age-specific prevalence of SARS-CoV-2 estimated for the Campania region, where about 9% of the overall population was estimated to have developed SARS-CoV-2 prior to the introduction of vaccination (Figure S24).

In the scenario with higher immunity, we initialized the population according to the age-specific prevalence of SARS-CoV-2 estimated for the Lombardy region, where about 23% of the overall population was estimated to have developed SARS-CoV-2 prior to the introduction of vaccination (Figure S25).

Results obtained in the baseline scenario are marginally affected by assumptions on initial immunity to SARS-CoV-2 (Figure S26).

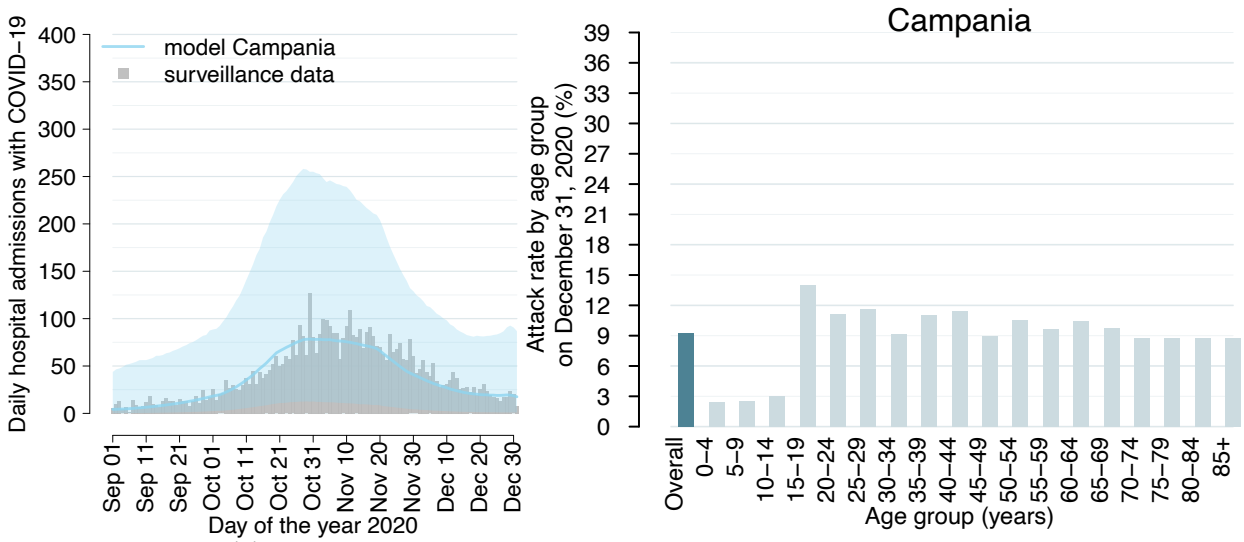

Figure S24. Scenario with lower immunity at vaccination start. Left: Daily hospitalizations with COVID-19 over time in the Campania region, according to surveillance data [22] (gray bars) and as estimated by the model [21] (solid line, median; shaded area, 95% CI). Right: Overall and age-specific fraction of population infected with SARS-CoV-2 in the Campania region at the beginning of the vaccination campaign (end of December 2020) [21].

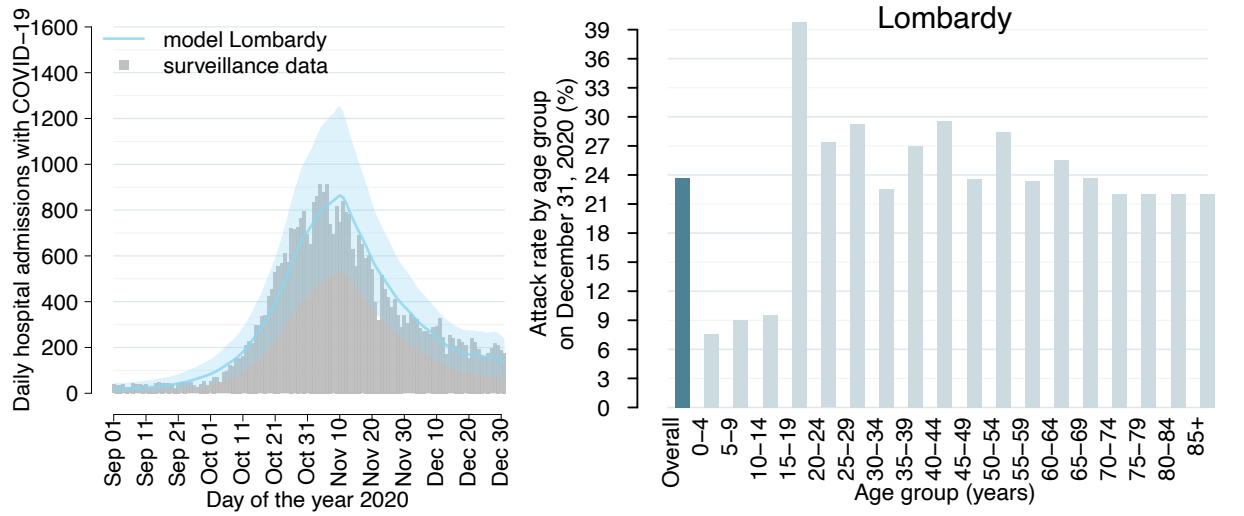

Figure S25. Scenario with higher immunity at vaccination start. Left: Daily hospitalizations with COVID-19 over time in the Lombardy region, according to surveillance data [22] (gray bars) and as estimated by the model [21] (solid line, median; shaded area, 95% CI). Right: Overall and age-specific fraction of population infected with SARS-CoV-2 in the Lombardy region at the beginning of the vaccination campaign (end of December 2020) [21].

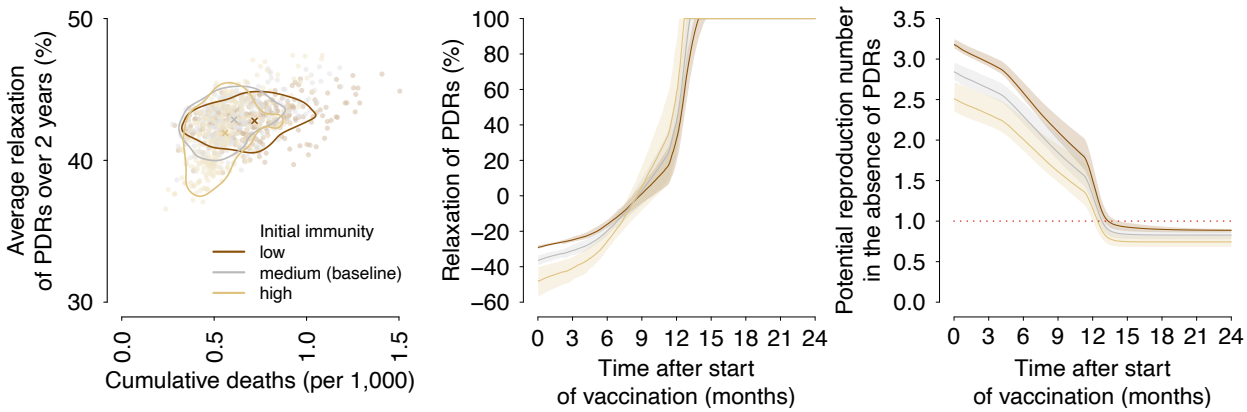

Figure S26. Alternative scenarios on initial immunity. Left: comparison between scenarios in terms of the cumulative incidence of deaths and the average relaxation of PDRs over the two simulated years. Individual stochastic simulations are shown as points, the mean of their bivariate distribution as crosses and its 75-percentile as closed curves. Center: relaxation of PDRs over time. Solid lines indicate the median, shaded areas the 95% projection interval. Right: potential reproduction number over time. Solid lines indicate the median, shaded areas the 95% projection interval. The horizontal dashed red line indicates the epidemic threshold.

References

1. Mossong J, Hens N, Jit M, Beutels P, Auranen K, Mikolajczyk R, et al. Social contacts and mixing patterns relevant to the spread of infectious diseases. PLoS Med. 2008 Mar 25;5(3):e74.
2. Mossong J, Hens N, Jit M, Beutels P, Auranen K, Mikolajczyk R, et al. POLYMOD social contact data 34 (Version 1.1, 2017) [Data set]. Zenodo. http://doi.org/10.5281/zenodo.1059920
3. Hu S, Wang W, Wang Y, Litvinova M, Luo K, Ren L, et al. Infectivity, susceptibility, and risk factors associated with SARS-CoV-2 transmission under intensive contact tracing in Hunan, China. Nat Commun. 2021 Mar 9;12(1):1-1. https://doi.org/10.1038/s41467-021-21710-6
4. Cereda D, Tirani M, Rovida F, Demicheli V, Ajelli M, Poletti P, et al. The early phase of the COVID-19 16 outbreak in Lombardy, Italy. ArXiv200309320 Q-Bio. 20 Mar 2020; Available at: 17 http://arxiv.org/abs/2003.09320
5. Riccardo F, Ajelli M, Andrianou XD, Bella A, Del Manso M, Fabiani M, et al. Epidemiological characteristics of COVID-19 cases and estimates of the reproductive numbers 1 month into the epidemic, Italy, 28 January to 31 March 2020. Euro Surveill. 2020;25(49):pii=2000790. https://doi.org/10.2807/1560-7917.ES.2020.25.49.2000790
6. Stefanelli P, Trentini F, Guzzetta G, Marziano V, Mammone A, Poletti P, et al. Co-circulation of SARS-CoV-2 variants B. 1.1. 7 and P. 1. medRxiv, 2021. Available at https://www.medrxiv.org/content/10.1101/2021.04.06.21254923v1
7. Davies NG, Abbott S, Barnard RC, Jarvis CI, Kucharski AJ, Munday JD, et al. Estimated transmissibility and impact of SARS-CoV-2 lineage B.1.1.7 in England. Science, 2021.
8. Volz E, Mishra S, Chand M, Barrett JC, Johnson R, Geidelberg L, et al. Assessing transmissibility of SARS-CoV-2 lineage B. 1.1. 7 in England. Nature. 2021 Mar 25:1-7.
9. Gaymard A, Bosetti P, Feri A, Destras G, Enouf V, Andronico A, et al. Early assessment of diffusion and possible expansion of SARS-CoV-2 Lineage 20I/501Y. V1 (B. 1.1. 7, variant of concern 202012/01) in France, January to March 2021. Euro Surveill 2021 Mar 4;26(9):2100133.
10. Galloway SE, Paul P, MacCannell DR, Johansson MA, Brooks JT, MacNeil A, et al. Emergence of SARS-CoV-2 B.1.1.7 lineage—United States, December 29, 2020 – January 12, 2021. Morbidity and Mortality Weekly Report. 2021 Jan 22;70(3):95.
11. Dagan N, Barda N, Kepten E, Miron O, Perchik S, Katz MA, et al. BNT162b2 mRNA Covid-19 vaccine in a nationwide mass vaccination setting. N Engl J Med. 2021 Feb 24. https://doi.org/10.1056/NEJMoa2101765.
12. Polack FP, Thomas SJ, Kitchin N, Absalon J, Gurtman A, Lockhart S, et al. Safety and efficacy of the BNT162b2 mRNA Covid-19 vaccine. N Engl J Med. 2020 Dec 31;383(27):2603-15.
13. Voysey M, Clemens SA, Madhi SA, Weckx LY, Folegatti PM, Aley PK, et al. Single-dose administration and the influence of the timing of the booster dose on immunogenicity and efficacy of ChAdOx1 nCoV-19 (AZD1222) vaccine: a pooled analysis of four randomised trials. The Lancet. 2021 Feb 19.

14. Thompson MG, Burgess JL, Naleway AL, et al. Interim Estimates of Vaccine Effectiveness of BNT162b2 and mRNA-1273 COVID-19 Vaccines in Preventing SARS-CoV-2 Infection Among Health Care Personnel, First Responders, and Other Essential and Frontline Workers — Eight U.S. Locations, December 2020–March 2021. MMWR Morb Mortal Wkly Rep 2021;70:495–500. DOI: http://dx.doi.org/10.15585/mmwr.mm7013e3external icon
15. Baden LR, El Sahly HM, Essink B, Kotloff K, Frey S, Novak R, et al. Efficacy and safety of the mRNA-1273 SARS-CoV-2 vaccine. N Engl J Med. 2021 Feb 4;384(5):403-16. https://www.nejm.org/doi/full/10.1056/NEJMoa2035389.
16. Diekmann O, Heesterbeek JA, Metz JA. On the definition and the computation of the basic reproduction ratio R0 in models for infectious diseases in heterogeneous populations. J Math Biol. 1990;28(4):365-82.
17. Diekmann O, Heesterbeek JA, Roberts MG. The construction of next-generation matrices for compartmental epidemic models. J R Soc Interface. 2010 Jun 6;7(47):873-85. https://doi.org/10.1098/rsif.2009.0386
18. Marziano V, Poletti P, Trentini F, Melegaro A, Ajelli M, Merler S. Parental vaccination to reduce measles immunity gaps in Italy. Elife. 2019 Sep 3;8:e44942.
19. Italian National Institute of Statistics. Popolazione residente per età, sesso e stato civile al 1 Gennaio 2020. http://demo.istat.it/pop2020/index.html. Accessed March 15, 2021.
20. Italian National Institute of Statistics. Indagine Multiscopo sulle famiglie: aspetti della vita quotidiana. http://dati.istat.it/Index.aspx?QueryId=15448# [Italian] Accessed March 15, 2021.
21. Marziano V, Guzzetta G, Rondinone BM, Boccuni F, Riccardo F, Bella A, et al. Retrospective analysis of the Italian exit strategy from COVID-19 lockdown. Proc Natl Acad Sci USA 118(4):e2019617118, 2021.
22. Istituto Superiore di Sanità. COVID-19 integrated surveillance data in Italy. https://www.epicentro.iss.it/coronavirus/sars-cov-2-dashboard
23. European Commission. A common approach to travel measures in the EU. https://ec.europa.eu/info/live-work-travel-eu/coronavirus-response/travel-during-coronavirus-pandemic/common-approach-travel-measures-eu_en Accessed March 15, 2021.
24. Poletti P, Tirani M, Cereda D, Trentini F, Guzzetta G, Marziano V, et al. Age-specific SARS-CoV-2 infection fatality ratio and associated risk factors, Italy, February to April 2020. Eurosurveill. 2020 Aug 6;25(31):2001383.
25. Trentini F, Marziano V, Guzzetta G, Tirani M, Cereda D, Poletti P, et al. Healthcare strain and intensive care during the COVID-19 outbreak in the Lombardy region: a retrospective observational study on 43,538 hospitalized patients. medRxiv. 2020 Jan 1.
26. Dipartimento di Protezione Civile, COVID-19 Italia - Monitoraggio situazione. https://github.com/pcm-dpc/COVID-19. Accessed March 15, 2021.
27. Trends of influenza vaccination campaigns in Italy: comparison between seasons 1999-2000/2019-2020 http://www.salute.gov.it/imgs/C_17_tavole_19_3_0_file.pdf [Italian] Accessed March 15, 2021.
28. Yang J, Marziano V, Deng X, Guzzetta G, Zhang J, Trentini F, et al. Can a COVID-19 vaccination program guarantee the return to a pre-pandemic lifestyle? Medrxiv. 2021 https://www.medrxiv.org/content/10.1101/2021.02.03.21251108v1.
29. WHO SAGE roadmap for prioritizing uses of COVID-19 vaccines in the context of limited supply. https://www.who.int/docs/default-source/immunization/sage/covid/sage-prioritization-roadmap-covid19-vaccines.pdf?Status=Temp&sfvrsn=bf227443_2. Accessed March 15, 2021.
30. Lazarus JV, Ratzan SC, Palayew A, Gostin LO, Larson HJ, Rabin K, et al. A global survey of potential acceptance of a COVID-19 vaccine. Nat Med. 2020:1-4.
31. Graffigna G, Palamenghi L, Boccia S, Barello S. Relationship between Citizens' Health Engagement and Intention to Take the COVID-19 Vaccine in Italy: A Mediation Analysis. Vaccines. 2020; 8(4):576. https://doi.org/10.3390/vaccines8040576
32. Barello S, Nania T, Dellafiore F, Graffigna G, Caruso R. 'Vaccine hesitancy' among university students in Italy during the COVID-19 pandemic. Eur J Epidemiol 2020.
33. Ministry of Health. Strategic Plan for COVID-19 vaccination. https://www.trovanorme.salute.gov.it/norme/renderNormsanPdf?anno=2021&codLeg=78657&parte=1%20&serie=null [Italian] Accessed April 15, 2021.
34. Italian National Institute of Statistics. Imprese – occupati. http://dati.istat.it/Index.aspx?DataSetCode=DICA_ASIAUE1P Accessed April 15, 2021.
35. Italian National Institute of Statistics. I presidi residenziali Socio-assistenziali e socio-sanitari. https://www.istat.it/it/files//2018/05/Presidi-residenziali_2015.pdf. Accessed April 15, 2021.

36. Ministry of Health. Stima della potenziale quantità di dosi di vaccino disponibili (in milioni) in Italia nel 2021, per trimestre e per azienda produttrice, in base ad accordi preliminari d'acquisto (APA) sottoscritti dalla Commissione europea e previa AIC (aggiornamento 3 marzo 2021). http://www.salute.gov.it/imgs/C_17_pagineAree_5452_4_file.pdf [Italian] Accessed April 15, 2021.
37. Challen R, Brooks-Pollock E, Read JM, Dyson L, Tsaneva-Atanasova K, Danon L. Risk of mortality in patients infected with SARS-CoV-2 variant of concern 202012/1: matched cohort study. BMJ 2021; 372:n579
38. Davies NG, Jarvis CI, CMMID COVID-19 Working Group, Edmunds WJ, Jewell NP, Diaz-Ordaz K, Keogh RH. Increased mortality in community-tested cases of SARS-CoV-2 lineage B.1.1.7. Nature, 2021; https://doi.org/10.1038/s41586-021-03426-1
39. Viner RM, Mytton OT, Bonell C, Melendez-Torres GJ, Ward J, Hudson L, et al. Susceptibility to SARS-CoV-2 infection among children and adolescents compared with adults: a systematic review and meta-analysis. JAMA Pediatr, 175(2), 143-156.